J. Fluid Mech. (2014), *vol.* 756, *pp.* 870–902.
doi:10.1017/jfm.2014.461

A stochastic model for the relative motion of high Stokes number particles in isotropic turbulence

Sarma L. Rani[1],†, Rohit Dhariwal[1] and Donald L. Koch[2]

[1]Mechanical and Aerospace Engineering Department, University of Alabama in Huntsville, Huntsville, AL 35899, USA

[2]School of Chemical and Biomolecular Engineering, Cornell University, Ithaca, NY 14853, USA

(Received 25 January 2014; revised 27 May 2014; accepted 6 August 2014; first published online 5 September 2014)

The probability density function (PDF) kinetic equation describing the relative motion of inertial particle pairs in a turbulent flow requires closure of the phase-space diffusion current. A novel analytical closure for the diffusion current is presented that is applicable to high-inertia particle pairs with Stokes numbers $St_r \gg 1$. Here St_r is a Stokes number based on the time scale τ_r of eddies whose size scales with pair separation r. In the asymptotic limit of $St_r \gg 1$, the pair PDF kinetic equation reduces to an equation of Fokker–Planck form. The diffusion tensor characterizing the diffusion current in the Fokker–Planck equation is equal to $1/\tau_v^2$ multiplied by the time integral of the Lagrangian correlation of fluid relative velocities along particle-pair trajectories. Here, τ_v is the particle viscous relaxation time. Closure of the diffusion tensor is achieved by converting the Lagrangian correlations of fluid relative velocities 'seen' by pairs into Eulerian fluid-velocity correlations at pair separations that remain essentially constant during time scales of $O(\tau_r)$; the pair centre of mass, however, is not stationary and responds to eddies with time scales comparable to or smaller than τ_v. For isotropic turbulence, Eulerian fluid-velocity correlations may be expressed as Fourier transforms of the velocity spectrum tensor, enabling us to derive a closed-form expression for the diffusion tensor. A salient feature of this closure is that it has a single, unique form for pair separations spanning the entire spectrum of turbulence scales, unlike previous closures that involve velocity structure functions with different forms for the integral, inertial subrange, and Kolmogorov-scale separations. Using this closure, Langevin equations, which are statistically equivalent to the Fokker–Planck equation, were solved to evolve particle-pair relative velocities and separations in stationary isotropic turbulence. The Langevin equation approach enables the simulation of the full PDF of pair relative motion, instead of only the first few moments of the PDF as is the case in a moments-based approach. Accordingly, PDFs $\Omega(U|r)$ and $\Omega(U_r|r)$ are computed and presented for various separations r, where the former is the PDF of relative velocity U and the latter is the PDF of the radial component of relative velocity U_r, both conditioned upon the separation r. Consistent with the direct numerical simulation (DNS) study of Sundaram & Collins (*J. Fluid Mech.*, vol. 335, 1997, pp. 75–109), the Langevin simulations capture the transition of $\Omega(U|r)$ from being Gaussian at integral-scale separations to an exponential PDF at Kolmogorov-scale separations. The radial distribution functions

†Email address for correspondence: sarma.rani@uah.edu

(RDFs) computed from these simulations also show reasonable quantitative agreement with those from the DNS study of Février, Simonin & Legendre (*Proceedings of the Fourth International Conference on Multiphase Flow, New Orleans*, 2001).

Key words: isotropic turbulence, multiphase and particle-laden flows, particle/fluid flows

1. Introduction

The two principal quantities describing particle-pair relative motion in a turbulent flow are: (i) the radial distribution function (RDF) which is a measure of the number density of particles that are located at a separation r from a reference particle, and (ii) the probability density function (PDF) of the relative velocities of particle pairs conditioned upon separation r. Both can be determined through direct numerical simulation (DNS) of particle-laden turbulent flows. However, DNS suffers from the well-known computational limitation on the Reynolds numbers that can be achieved. This drawback of DNS is one of the motivating factors for developing PDF-equation-based stochastic models for particle-laden turbulent flows. The transport equation for the PDF of pair separation and relative velocity vectors, $\boldsymbol{r}$ and $\boldsymbol{U}$ respectively, contains an unclosed phase-space diffusion current. In this study, a novel closure is derived for the diffusion current in the limit of Stokes number $St_r \gg 1$ when the pair PDF equation reduces to the Fokker–Planck form. Here St_r is the Stokes number based on the time scale τ_r of eddies whose size is of the order of pair separation r. Predictions of RDF and relative velocity PDF obtained from this closure show good agreement with prior DNS results.

Numerous computational and theoretical studies of inertial particle motion in isotropic turbulence have established that dense particles with response time (τ_v) of the order of the Kolmorogorov time scale (τ_η) preferentially accumulate in regions of excess strain over vorticity (Maxey 1987; Squires & Eaton 1991; Eaton & Fessler 1994; Druzhinin 1995; Druzhinin & Elghobashi 1999; Ferry & Balachandar 2001; Ferry, Rani & Balachandar 2003; Rani & Balachandar 2003; Chun *et al.* 2005; Ray & Collins 2011). When $\tau_v \lesssim \tau_\eta$, particle accumulation occurs at separations smaller than the Kolmogorov length scale (η). Preferential concentration at separations of $O(\eta)$ is maximized for particles with Stokes number $St_\eta \sim O(1)$, and is attenuated when $St_\eta > 1$, where $St_\eta = \tau_v/\tau_\eta$. Février, Simonin & Legendre (2001) found that particles with $St_\eta > 1$ also exhibit preferential concentration, as quantified by RDF values greater than unity, but the peak in the RDF shifts towards separations larger than η for higher St_η.

Turbulence-induced clustering of high-inertia particles has potential applications in many astrophysical environments, such as the interstellar medium, protoplanetary disks, and the atmospheres of planets and dwarf stars (Chiang & Youdin 2005; Pan *et al.* 2011). A phenomenon of significant interest in astrophysics is the formation of planetesimals from dust particles in protoplanetary disks. An intriguing possibility that astrophysicists are investigating is whether gas-turbulence-driven dispersion, sedimentation, collisional coalescence and fragmentation of dust particles play an important role in the formation of planetesimals. Particle preferential concentration at separations in the inertial subrange is of particular interest to the problem of planetesimal formation, where the Stokes numbers of relevance are estimated to be $St_\eta \sim 10$–100 (Pan *et al.* 2011). The proposed high-Stokes-number theory would be directly applicable in this scenario.

In a DNS study of inertial particle dynamics in isotropic turbulence by Sundaram & Collins (1997), it was observed that the PDF of particle-pair relative velocity was Gaussian at pair separations of the order of the turbulent integral length scale, and that this PDF became increasingly non-Gaussian (exponential) as the separation decreased. Particle motion at smaller separations (compared to, say, the integral length scale) will be strongly correlated due to the influence of the fluid, giving rise to the non-Gaussian relative velocity PDF. At larger separations, particles will be less correlated because turbulent fluctuations effectively behave like Gaussian white noise, leading to a Gaussian relative velocity PDF.

The motion of disperse particles in turbulent flows is inherently stochastic due to the turbulence-driven random fluctuating forces acting on the particles. Hence, a PDF-equation-based approach presents a natural avenue to study particle-laden turbulent flows. However, this approach poses a closure problem in the form of a diffusion-current term that arises when one averages the phase-space density (PSD) equation over an ensemble of particle initial conditions and flow realizations. Reeks (1980, 1991, 1992, 2005) and Hyland, McKee & Reeks (1999) are among the seminal fundamental studies on the PDF kinetic equation approach to model particle transport in turbulent flows.

The PDF kinetic equation approach of Reeks and coworkers considered the single-particle PDF $\langle P(\boldsymbol{v}, \boldsymbol{x}; t)\rangle$ whose phase space consists of particle velocity and position vectors $\boldsymbol{v}$ and $\boldsymbol{x}$, respectively. In Reeks (1980), the Eulerian direct interaction (EDI) approximation (Kraichnan 1961) was used to close the diffusion-current term. In a subsequent study, Reeks (1991) showed that in order to preserve invariance to a random Galilean transformation (RGT), the diffusion current should be of the following form:

$$\boldsymbol{j} = -\left(\frac{\partial}{\partial \boldsymbol{v}} \cdot \boldsymbol{\mu} + \frac{\partial}{\partial \boldsymbol{x}} \cdot \boldsymbol{\lambda} + \boldsymbol{\gamma}\right) \langle P(\boldsymbol{v}, \boldsymbol{x}; t)\rangle \tag{1.1}$$

where $\boldsymbol{j}$ represents the phase-space diffusion current, $\boldsymbol{\mu}$ and $\boldsymbol{\lambda}$ are diffusion tensors, and $\boldsymbol{\gamma}$ is a drift vector. In an improvement over Reeks (1980), Reeks (1991) derived a closure for the diffusion current in the particle PDF equation by using Kraichnan's Lagrangian-history direct interaction (LHDI) approximation (Kraichnan 1965) in conjunction with a renormalized perturbation theory. One of the important advantages of LHDI is that it preserves RGT invariance. Subsequently, Hyland *et al.* (1999) adopted the Furutsu–Novikov–Donsker (FND) formula to derive closed-form expressions for the two diffusion terms in (1.1).

In an important theoretical study, Pozorski & Minier (1999) discussed the significance of the choice of state variables in the PDF-equation-based modelling of two-phase flows. They presented two broad formulations depending upon the choice of the state vector. The first formulation considered a state space that included only the particle position and velocity, $\boldsymbol{x}$ and $\boldsymbol{v}$ respectively. This is a traditional approach that is used in Reeks (1991) and Hyland *et al.* (1999), as well as in the current study (although we consider relative quantities and not single-particle quantities). The first approach gives rise to a diffusion-current closure of the form in (1.1). In the second approach, the state vector also includes the fluid velocity 'seen' by the particles, $\boldsymbol{u}$. Inclusion of $\boldsymbol{u}$ in the state vector necessitates a Langevin evolution equation of the form $\mathrm{d}\boldsymbol{u}/\mathrm{d}t = \boldsymbol{A}$. The PDF equation for the enlarged state space, $(\boldsymbol{x}, \boldsymbol{v}, \boldsymbol{u})$, now has a new unknown term $\langle \boldsymbol{A}|\boldsymbol{x}, \boldsymbol{v}, \boldsymbol{u}\rangle$. To achieve closure, Pozorski & Minier (1999) proposed a Langevin model for the time evolution of the 'seen' fluid velocity.

Gardiner (1990), and subsequently Pozorski & Minier (1999), observed that one retains the temporally slowly varying quantities in the state vector, while removing

the quickly varying ones. Gardiner (1990) demonstrated that in dynamical systems characterized by widely separated time scales, one is typically not interested in system variations occurring on very short time scales, and refers to such variables as 'fast variables'. He further says that fast variables are effectively slaved by slow variables, meaning that by the time the latter have relaxed to a steady state, the fast variable values can simply be determined using the steady-state values of the slow variables. Pozorski & Minier (1999) discuss the replacement of removed fast variables with models containing their equilibrium values along with white-noise terms.

The preceding discussion is directly applicable to the current study, where the reference time scale is the particle viscous relaxation time, τ_v. This means that the particle variables of interest such as the pair separation and relative velocity vary over times $\sim\tau_v$. In the asymptotic limit of Stokes number $St_r = \tau_v/\tau_r \gg 1$, where τ_r is the time scale of an eddy whose size scales with separation r, the fluid time scales having an impact on the pair relative motion are much smaller than τ_v, and hence the seen fluid relative velocity is a fast variable. This justifies the elimination of the seen fluid relative velocity $\Delta\boldsymbol{u}$ from the state vector. In this context, it is also relevant to discuss the study by Reeks (2005). In that study, Reeks rigorously examined the purported differences between the above two approaches to stochastic modelling of particle-laden flows: the kinetic PDF model (KM) pioneered by Reeks, and the generalized Langevin model (GLM) pioneered by Simonin, Deutsch & Minier (1993) and Pozorski & Minier (1999). The principal differences between KM and GLM are with regard to the non-inclusion or inclusion, respectively, of $\boldsymbol{u}$ in the state vector, and the different closure requirements this entails (note that Reeks was considering single-particle dynamics). Reeks asserted that KM and GLM will, in principle, give identical results provided the modelling inputs to both approaches are the same. For instance, integrating the GLM PDF equation over all the fluid velocities local to the particles will yield an equation that is identical to the KM PDF equation. However, if the closures for the unknown terms in the two approaches are fundamentally different, then the closed PDF equations for the two approaches, and thereby their predictions, will differ. Reeks demonstrated that the differences between the two approaches can be attributed to the neglect of the inertial convection term in the GLM equation for the mean carrier flow velocity seen by the particle.

Pozorski & Minier (1999) elucidate the implications of the choice of the state vector in the KM approach, and more importantly, the properties of the PDF kinetic equation resulting from such a choice. This equation has a form that is apparently analogous to the Fokker–Planck equation. Reeks (1991), however, shows that the PDF equation becomes the classical Fokker–Planck equation only for asymptotically large particle Stokes numbers when one may represent the underlying turbulence as white noise. Pozorski & Minier (1999) bring out a more crucial difference between the PDF kinetic equation and the Fokker–Planck equation. This difference relates to the fact that in the kinetic equation, the diffusion block matrix $\boldsymbol{B}$ formed from the diffusion tensors $\boldsymbol{\lambda}$ and $\boldsymbol{\mu}$ (see (1.1)) is not positive definite, whereas for the classical Fokker–Planck equation $\boldsymbol{B}$ is positive definite. This would mean that $\boldsymbol{B}$ for the kinetic equation has at least one negative eigenvalue so the effects of turbulence on particles for that eigenvalue are manifested as 'antidiffusion' behaviour in the phase space. Since the current study specifically considers the asymptotic limit of $St_r \gg 1$, the PDF equation reduces to the classical Fokker–Planck equation for the PDF of pair separation and relative velocity.

In their encyclopaedic monograph, Minier & Peirano (2001) provide an overview of the PDF methods for studying particle-laden turbulent flows. For instance, the principle of the elimination of fast variables from the state vector is illustrated in

detail, and provides the basis for the removal of the 'seen' fluid relative velocity $\Delta \boldsymbol{u}$ from the state vector in the current study. They also show that the effects of the eliminated fast variable may be modelled as a white-noise term represented using a Wiener increment in the stochastic differential equation or the Langevin equation governing the slow variable. The relevant slow variable in the present study is the pair relative velocity $\boldsymbol{U}$, whose Langevin evolution equation contains a white-noise term modelling the effects of the underlying fluid turbulence on pair relative velocity. The consequence of the white-noise representation is that this term is manifested as a phase-space diffusion current characterized by a diffusion tensor in the Fokker–Planck equation governing the PDF of pair relative motion.

In a precursor study to the current one, Zaichik & Alipchenkov (2003) developed a stochastic model based on the kinetic equation for the joint PDF of pair separation and relative velocity. Although the current study and Zaichik & Alipchenkov (2003) are similar in this respect, i.e. a stochastic investigation of particle-pair relative motion, there are important fundamental distinctions between the two studies. The principal difference lies in the approach adopted to close the diffusion current in the PDF equation. Zaichik & Alipchenkov (2003) achieved closure by using the FND formula wherein the diffusion current was expressed in terms of the second-order cumulants (or moments) of the fluid relative velocities 'seen' by the inertial particle pairs. Swailes & Darbyshire (1997) showed that the diffusion current, in principle, can be written as an infinite series expansion comprising fluid velocity cumulants of all integral orders. The FND formula is a special case of this generalized expansion, where only the first- and second-order cumulants are non-zero, and all others are exactly zero (due to the Gaussian random function assumption inherent to FND). For isotropic turbulence, the first-order cumulant is also zero. Therefore, the assumption implicit in Zaichik & Alipchenkov (2003) is that the fluid relative velocities are Gaussian. This assumption is reasonable for large-scale eddies driving the relative motion of pairs at integral-scale separations (Batchelor 1953). But, it is questionable at separations in the inertial and dissipative subranges. The increasing non-Gaussianity of the relative velocities of fluid particles as their separations approached the Kolmogorov scale was discussed by Minier & Peirano (2001). This was also confirmed by the DNS of Gualtieri *et al.* (2002) who showed that the PDF of fluid relative velocity at a separation $r/\eta = 8$ is Gaussian only for small values of relative velocity, and that the PDF quickly deviates away from being Gaussian at larger values. The current study does not use the FND formula to achieve closure, but is based on a perturbation analysis of the pair PDF equation.

Using the FND formula, Zaichik & Alipchenkov (2003) expressed the particle–eddy interaction (diffusion current) term in the PDF equation as a combination of: (i) a diffusion term in the relative velocity space, and (ii) a cross-diffusion term in the separation–relative-velocity space. Both the diffusion terms contain the time integral of the two-point, two-time Lagrangian correlation of fluid relative velocities along pair trajectories. In order to close these correlations, they further assumed that the correlation of fluid relative velocities along inertial-pair trajectories is the same as that along fluid-pair trajectories. It is evident that this assumption is appropriate only for Stokes number $St < 1$ when one may assume that the deviation in the trajectories of inertial and fluid particles is not significant. Therefore, the Zaichik & Alipchenkov (2003) theory is most appropriate for small-Stokes-number particles. In the current study, we consider high-St particles, which enables us to develop an alternative closure for the Lagrangian correlations. This is the second major difference between the two studies.

Another important difference concerns the simulation approach adopted in the two studies. In order to predict pair dispersion and particle preferential accumulation in isotropic turbulence, Zaichik & Alipchenkov (2003) solved the governing equations for the zeroth, first and second relative-velocity moments of the pair PDF. These moments equations were derived from the fully closed pair PDF equation, but they all contain unclosed higher-order moment terms. In the current study, we simulate the Langevin equations, which are equivalent to the Fokker–Planck equation in a weak sense, to evolve the relative velocity and separation vectors of a large number of particle pairs. When compared to solving a finite number of PDF moments equations, the Langevin approach is higher-order accurate in the sense that the Langevin simulations inherently include all moments of the pair PDF. Another advantage of this approach is that it allows us to explicitly compute the PDFs of pair relative velocity at various separations, thereby enabling us to track the transition in the nature of the PDF as the separations are reduced from the order of integral scale to Kolmogorov scale. The moments-equations-based approach also presents the conundrum of additional closure problems since an equation for a given moment contains the next higher-order moment. This leads to a chain of an infinite number of equations, which is typically broken by assuming that the moments of a certain order or higher are zero. For example, in Zaichik & Alipchenkov (2003), fourth- and higher-order moments are set to zero, and the third-order moments are closed in terms of the second moments using the gradient transport approximation which is likely to be quite poor when the relative-velocity PDF is far from Gaussian as we find it is. This problem is completely obviated through the Langevin equations approach since there are no additional closure issues.

Finally, the two studies also differ in the state vectors that they consider in order to derive the final form of the pair PDF equation. Zaichik & Alipchenkov (2003) considered a state vector comprising only the pair separation and relative velocity, $\boldsymbol{r}$ and $\boldsymbol{U}$, respectively. The current study begins with the high-dimensional PDF $P(\boldsymbol{r}, \boldsymbol{U}, \boldsymbol{x}, \boldsymbol{V}; t)$, where the state vector includes the particle-pair centre-of-mass position and velocity $\boldsymbol{x}$ and $\boldsymbol{V}$, respectively, in addition to $\boldsymbol{r}$ and $\boldsymbol{U}$. The need to include $\boldsymbol{x}$ and $\boldsymbol{V}$ arises naturally since we do not approximate inertial-pair trajectories to be the same as fluid-pair trajectories. The state vector $(\boldsymbol{r}, \boldsymbol{U}, \boldsymbol{x}, \boldsymbol{V})$ allows one to account for not only the relative motion of a particle pair, but also the dynamics of the pair center-of-mass. The inclusion of $\boldsymbol{x}$ and $\boldsymbol{V}$ in the state space has an important benefit in that it enables us to determine the orders of magnitude of the various terms representing the dynamics of the centre of mass in the P equation. The order-of-magnitude information will help us identify the conditions under which certain terms may be neglected when performing a perturbation analysis of the PDF equation. For instance, we incorporate into the diffusion coefficient tensor the effects of change in $\boldsymbol{x}$ during integral time scales due to the velocity $\boldsymbol{V}$ through the relative velocity vector $\boldsymbol{W} = \boldsymbol{u}_I - \boldsymbol{V}$. Here $\boldsymbol{u}_I$ is the velocity with which eddies of size r are passively advected past the centre of mass by the large-scale eddies (cf. (2.26)–(2.29) below).

Using the RDFs, Zaichik & Alipchenkov (2003) demonstrated that high-St_η particles show preferential concentration at length scales that are much larger than η, and are scaled by the integral length scale (L). Their study also predicts that for $St_\eta \geqslant 4$, the RDF plateaus (i.e. nearly zero slope in a log–log plot) for separations smaller than some multiples of the Kolmogorov length scale. For $St_\eta = 10$, Zaichik & Alipchenkov (2003) show a plateauing of the RDF for separations $r \lesssim 10\eta$. In contrast, our theory predicts the plateauing of the RDF to begin at smaller separations $r \sim \eta$ for $St_\eta = 10$, which is consistent with the DNS of Pan *et al.* (2011).

In a stochastic and computational study, Chun *et al.* (2005) studied particle relative motion in the limit of $St_\eta \ll 1$. This study was concerned with particle-pair separations smaller than the Kolmogorov length scale, where the pair relative motion is principally determined by the dissipation range of the turbulent energy spectrum. They also assumed a locally linear flow for the fluid velocity difference along the pair trajectory. Using a state space comprising only the pair separation vector $\boldsymbol{r}$, they derived the PDF equation consisting of drift and diffusion terms. The closure of the two terms involved expanding the pair relative velocity, $\boldsymbol{w}$, as a perturbation expansion in Stokes number (St_η), and retaining only the zeroth- and first-order terms in St_η. This results in a drift velocity $\sim St_\eta^2$, and a diffusion coefficient $\sim r^2$, where r is the particle separation.

Pan & Padaon (2010) derived an analytical model for the relative velocity of both monodisperse and bidisperse inertial particles in turbulent flows. Their objective was to derive a model that captures particle relative motion for all particle response times, i.e. $\tau_v \ll \tau_\eta$, $\tau_v \gg \tau_I$, as well as $\tau_\eta \lesssim \tau_v \lesssim \tau_I$. Here τ_I is the integral time scale. Their model is conceptually based on the approach of Ayala, Rosa & Wang (2008). However, Ayala *et al.* (2008) only considered particle separation due to gravity for sedimenting droplets in turbulent flows, and neglected particle relative motion due to turbulent dispersion. When developing an analytical model for particle relative velocity that includes turbulent dispersion, one invariably encounters two-point two-time correlations of fluid relative velocities along pair trajectories. As was done in earlier studies (Hyland *et al.* 1999; Zaichik & Alipchenkov 2003; Zaichik, Simonin & Alipchenkov 2003; Derevich 2006; Zaichik, Simonin & Alipchenkov 2006), Pan & Padaon (2010) approximated these correlations as being those along fluid-particle-pair trajectories. In this respect, our study differs from these studies in that fluid relative-velocity correlations along inertial-pair trajectories are converted, in the limit of high Stokes number, into Eulerian two-point fluid velocity correlations.

Goswami & Kumaran (2010*a*,*b*) performed both DNS and Langevin stochastic simulations of high-Stokes-number particle dynamics in a turbulent Couette flow. In their stochastic model, they began by considering the Boltzmann equation for the particle fluctuating velocity PDF, which is reduced to a Fokker–Planck equation. However, the derivation behind modelling particle–eddy interactions as a Fokker–Planck-type diffusion term was not provided. It is important to note that the assumption that allows one to derive the Fokker–Planck equation is that the particle response time is much greater than the decay time for the fluid velocity fluctuations. In their Langevin simulations, the stochastic forcing term, $\boldsymbol{F}(t)$, is modelled as Gaussian white noise with zero mean and a second moment given by $\langle F_i(t)F_j(t')\rangle = 2D_{ij}\delta(t-t')$, where D_{ij} is the diffusion coefficient tensor in the particle velocity space (in the current study, diffusion coefficient is in the pair relative-velocity space). Diffusion coefficient, D_{ij}, is expressed in terms of a time integral of the Lagrangian fluid velocity correlation tensor. They, however, do not derive an explicit expression for the diffusion coefficient, and instead compute it using the fluid velocity autocorrelation data obtained from their DNS.

In a notable recent study, Bragg, Swailes & Skartlien (2012) performed a first-principles-based comparison of three well-known approaches for closing the diffusion current in the particle PDF kinetic equation. They are the FND method, LHDI of Reeks (1980), and van Kampen's operator representation technique (Pozorski & Minier 1999). Specifically, they investigated whether the closures obtained from these approaches are all equivalent, as is commonly accepted. Through a remarkably fundamental analysis of the implications of these approaches, they prove that the

equivalence breaks down in two scenarios: (i) when the underlying turbulence is inhomogeneous, and (ii) when the particles are inertialess, i.e. fluid particles, in which case the zero-drift or the fully mixed condition should be recovered. It is seen that only the FND method provides a closure that satisfies the zero-drift condition in both homogeneous and inhomogeneous incompressible systems.

In the current study, starting with the high-dimensional PDF equation governing the relative and correlated motion of particle pairs, we derive the transport equation for the PDF $\Omega(\boldsymbol{r}, \boldsymbol{U})$ of pair separation ($\boldsymbol{r}$) and relative velocity ($\boldsymbol{U}$) of high-Stokes-number particles. The transport equation for $\Omega(\boldsymbol{r}, \boldsymbol{U})$, which is of the Fokker–Planck type, contains a diffusion coefficient tensor that can be expressed as $1/\tau_v^2$ times the time integral of the Lagrangian correlation of fluid relative velocities along the pair trajectory. These Lagrangian correlations also need to be closed. One way to overcome this closure problem is to perform DNS of particle-laden turbulence and collect the correlation statistics. A different approach would be to develop a theoretical closure, which would necessitate certain assumptions. For example, in Zaichik & Alipchenkov (2003), the Lagrangian correlations are assumed to be correlations along fluid-particle trajectories. This assumption, however, is most appropriate in the limit of small particle Stokes number. In the current study, we begin by developing an alternative closure in the limit of $St_I \gg 1$ and $St_r \gg 1$. Here St_I and St_r are the Stokes numbers based on the integral time scale τ_I and the time scale τ_r of an eddy of size r, respectively. Subsequently, the closure is extended to $St_I \lesssim 1$ particles by accounting for the motion of the pair centre of mass. It is to be noted that the $St_r \gg 1$ requirement is much less stringent than $St_I \gg 1$. Finally, in the limit of $St_r \gg 1$ but $St_I \lesssim 1$, the Lagrangian two-point, two-time correlation is systematically converted first into an Eulerian two-time correlation, and subsequently into an Eulerian two-point correlation. For isotropic turbulence, these Eulerian velocity correlations can be conveniently expressed as Fourier transforms of the velocity spectrum tensor.

After deriving the closure for the diffusion tensor, the Fokker–Planck equation is solved in a weak sense by solving the corresponding Langevin equations to evolve the relative velocity and separation vectors of a large number of particle pairs. The Langevin simulations, also referred to as Monte-Carlo simulations, may be contrasted with an approach in which the governing equations for the first few moments of the PDF are derived and solved. The latter approach was adopted in Zaichik & Alipchenkov (2003).

The paper is organized as follows: § 2 presents the complete theoretical basis of this study. Section 3 discusses the Langevin-equation-based simulations used to compute the relative velocity PDFs, and the RDFs. Results from the Langevin equation simulations are presented and their implications discussed in § 4.

2. Theory

In § 2.1, the particle-pair PSD equation along with the pair Lagrangian governing equations are presented. In § 2.2, the PSD equation is shown to reduce to the Fokker–Planck equation in the limit of $St_r \gg 1$. Closure is developed for the diffusion tensor, which is then extended to $St_I \lesssim 1$ particles through a finite-St_I model for the relative velocity $\boldsymbol{W}$ between the fluid eddies (that are advected past the particle pair by integral-scale eddies) and the pair centre of mass; the expression for W_{rms}, the root mean square (r.m.s.) of $\boldsymbol{W}$, needed for this extension is derived in § 2.4.

2.1. *Phase-space density (PSD) equation*

For a dispersion of high-Stokes-number particles in stationary homogeneous isotropic turbulence, we consider the PSD, $P(\boldsymbol{R}_1, \boldsymbol{R}_2, \boldsymbol{U}_1, \boldsymbol{U}_2; t)$, that two particles take phase-space positions and velocities $\boldsymbol{R}_1$ and $\boldsymbol{R}_2$, and $\boldsymbol{U}_1$ and $\boldsymbol{U}_2$, respectively. The two-particle PSD is equivalent to $P(\boldsymbol{r}, \boldsymbol{U}, \boldsymbol{x}, \boldsymbol{V}; t)$, which is the PSD of a particle pair with separation $\boldsymbol{r}$, relative velocity $\boldsymbol{U}$, centre-of-mass position $\boldsymbol{x}$, and centre-of-mass velocity $\boldsymbol{V}$. The current notation, definition, and significance of the PSD are discussed in the appendix. The relative motion of particle pairs will depend not only on their separation and relative velocity vectors, but also on the dynamics of the pair centre of mass that can influence the way the pair samples the fluid velocity field. Conservation of PSD P yields:

$$\frac{\partial P}{\partial t} + \boldsymbol{\nabla}_{\boldsymbol{r}} \cdot (\dot{\boldsymbol{r}} P) + \boldsymbol{\nabla}_{\boldsymbol{U}} \cdot (\dot{\boldsymbol{U}} P) + \boldsymbol{\nabla}_{\boldsymbol{x}} \cdot (\dot{\boldsymbol{x}} P) + \boldsymbol{\nabla}_{\boldsymbol{V}} \cdot (\dot{\boldsymbol{V}} P) = 0 \tag{2.1}$$

where $\boldsymbol{\nabla}_{\boldsymbol{r}}$, $\boldsymbol{\nabla}_{\boldsymbol{x}}$, $\boldsymbol{\nabla}_{\boldsymbol{U}}$, and $\boldsymbol{\nabla}_{\boldsymbol{V}}$ represent gradients with respect to the corresponding variables.

The governing equations for $\boldsymbol{r}$, $\boldsymbol{U}$, $\boldsymbol{x}$, and $\boldsymbol{V}$ are:

$$\frac{\mathrm{d}\boldsymbol{r}}{\mathrm{d}t} = \boldsymbol{U}, \tag{2.2}$$

$$\frac{\mathrm{d}\boldsymbol{U}}{\mathrm{d}t} = -\frac{1}{\tau_v}\left[\boldsymbol{U}(t) - \Delta\boldsymbol{u}(\boldsymbol{r}, \boldsymbol{x}, t)\right], \tag{2.3}$$

$$\frac{\mathrm{d}\boldsymbol{x}}{\mathrm{d}t} = \boldsymbol{V}, \tag{2.4}$$

$$\frac{\mathrm{d}\boldsymbol{V}}{\mathrm{d}t} = -\frac{1}{\tau_v}\left[\boldsymbol{V}(t) - \frac{\boldsymbol{u}(\boldsymbol{R}_1(t), t) + \boldsymbol{u}(\boldsymbol{R}_2(t), t)}{2}\right] = -\frac{1}{\tau_v}\left[\boldsymbol{V}(t) - \boldsymbol{u}_{cm}(\boldsymbol{R}_1(t), \boldsymbol{R}_2(t), t)\right], \tag{2.5}$$

where τ_v is the particle response time, $\Delta\boldsymbol{u}(\boldsymbol{r}, \boldsymbol{x}, t) = [\boldsymbol{u}(\boldsymbol{R}_2(t), t) - \boldsymbol{u}(\boldsymbol{R}_1(t), t)]$ is the fluid relative velocity along the pair trajectory, and $\boldsymbol{u}_{cm}(\boldsymbol{R}_1(t), \boldsymbol{R}_2(t), t) = [\boldsymbol{u}(\boldsymbol{R}_1(t), t) + \boldsymbol{u}(\boldsymbol{R}_2(t), t)]/2$. Here $\boldsymbol{u}_{cm}$ may be interpreted as the fluid velocity influencing the dynamics of the pair centre of mass, but is not the fluid velocity at the centre-of-mass location. The velocity $\boldsymbol{u}_{cm}$ can be determined from $\boldsymbol{x}$ and $\boldsymbol{r}$ since $\boldsymbol{R}_2 = \boldsymbol{x} + (\boldsymbol{r}/2)$ and $\boldsymbol{R}_1 = \boldsymbol{x} - (\boldsymbol{r}/2)$. In (2.3) and (2.5), we assume that the fluid drag force is the predominant force acting on the particles and that the Stokes drag law is valid. Accordingly, the particle response time is defined as $\tau_v = \rho_p d_p^2/18\mu$, where ρ_p is the particle density, d_p is the particle diameter, and μ is the dynamic viscosity of the fluid.

Substituting (2.2)–(2.5) into (2.1) yields

$$\frac{\partial P}{\partial t} + \boldsymbol{\nabla}_{\boldsymbol{r}} \cdot (\boldsymbol{U}P) + \boldsymbol{\nabla}_{\boldsymbol{x}} \cdot (\boldsymbol{V}P) - \frac{1}{\tau_v}\boldsymbol{\nabla}_{\boldsymbol{U}} \cdot (\boldsymbol{U}P) - \frac{1}{\tau_v}\boldsymbol{\nabla}_{\boldsymbol{V}} \cdot (\boldsymbol{V}P) + \frac{1}{\tau_v}\boldsymbol{\nabla}_{\boldsymbol{U}} \cdot (\Delta\boldsymbol{u}P) + \frac{1}{\tau_v}\boldsymbol{\nabla}_{\boldsymbol{V}} \cdot (\boldsymbol{u}_{cm}P) = 0. \tag{2.6}$$

2.2. *Perturbation analysis*

In this section, the PSD equation (2.6) is transformed into a Fokker–Planck equation under the condition that the changes in pair relative velocity during the correlation

times of eddies that have an impact on their relative motion are small compared to the pair relative velocity itself. To model pair–eddy interactions as a Fokker–Planck-type diffusion term, we begin by averaging (2.6) over an ensemble of flow realizations, giving us:

$$\frac{\partial\langle P\rangle}{\partial t}+\boldsymbol{\nabla}_{\boldsymbol{r}}\cdot(\boldsymbol{U}\langle P\rangle)+\boldsymbol{\nabla}_{\boldsymbol{x}}\cdot(\boldsymbol{V}\langle P\rangle)-\frac{1}{\tau_v}\boldsymbol{\nabla}_{\boldsymbol{U}}\cdot(\boldsymbol{U}\langle P\rangle)-\frac{1}{\tau_v}\boldsymbol{\nabla}_{\boldsymbol{V}}\cdot(\boldsymbol{V}\langle P\rangle)+\frac{1}{\tau_v}\boldsymbol{\nabla}_{\boldsymbol{U}}\cdot\langle\Delta\boldsymbol{u}P\rangle+\frac{1}{\tau_v}\boldsymbol{\nabla}_{\boldsymbol{V}}\cdot\langle\boldsymbol{u}_{cm}P\rangle=0 \tag{2.7}$$

where $\langle\cdot\rangle$ represents ensemble averaging, and the terms $\langle\Delta\boldsymbol{u}P\rangle$ and $\langle\boldsymbol{u}_{cm}P\rangle$ represent turbulence–particle interactions. Since $\boldsymbol{U}$ and $\boldsymbol{V}$ are independent variables (like time t), $\langle\boldsymbol{U}P\rangle=\boldsymbol{U}\langle P\rangle$ and $\langle\boldsymbol{V}P\rangle=\boldsymbol{V}\langle P\rangle$.

As a first step toward modelling $\langle\Delta\boldsymbol{u}P\rangle$ and $\langle\boldsymbol{u}P\rangle$, consider

$$\langle\Delta\boldsymbol{u}P\rangle=\langle\Delta\boldsymbol{u}(\langle P\rangle+P')\rangle=\langle\Delta\boldsymbol{u}P'\rangle \tag{2.8}$$

where we have used the relations: $P=\langle P\rangle+P'$, and $\langle\Delta\boldsymbol{u}\rangle=0$ for isotropic turbulence. Here, P' is a fluctuation in P from the PDF $\langle P\rangle$. Similarly, $\langle\boldsymbol{u}_{cm}P\rangle=\langle\boldsymbol{u}_{cm}P'\rangle$.

We will show that in the limit of high Stokes number, we can express the last two terms of (2.7) as Fokker–Planck-type diffusion terms. Substituting $P=\langle P\rangle+P'$ into (2.6), and moving terms containing $\langle P\rangle$ to the right-hand side, we get:

$$\begin{aligned}&\frac{\partial P'}{\partial t}+\boldsymbol{\nabla}_{\boldsymbol{r}}\cdot(\boldsymbol{U}P')+\boldsymbol{\nabla}_{\boldsymbol{x}}\cdot(\boldsymbol{V}P')-\frac{1}{\tau_v}\boldsymbol{\nabla}_{\boldsymbol{U}}\cdot(\boldsymbol{U}P')-\frac{1}{\tau_v}\boldsymbol{\nabla}_{\boldsymbol{V}}\cdot(\boldsymbol{V}P')\\&\quad+\frac{1}{\tau_v}\boldsymbol{\nabla}_{\boldsymbol{U}}\cdot(\Delta\boldsymbol{u}P')+\frac{1}{\tau_v}\boldsymbol{\nabla}_{\boldsymbol{V}}\cdot(\boldsymbol{u}_{cm}P')\\&=-\left[\frac{\partial\langle P\rangle}{\partial t}+\boldsymbol{\nabla}_{\boldsymbol{r}}\cdot(\boldsymbol{U}\langle P\rangle)+\boldsymbol{\nabla}_{\boldsymbol{x}}\cdot(\boldsymbol{V}\langle P\rangle)-\frac{1}{\tau_v}\boldsymbol{\nabla}_{\boldsymbol{U}}\cdot(\boldsymbol{U}\langle P\rangle)-\frac{1}{\tau_v}\boldsymbol{\nabla}_{\boldsymbol{V}}\cdot(\boldsymbol{V}\langle P\rangle)\right.\\&\quad\left.+\frac{1}{\tau_v}\boldsymbol{\nabla}_{\boldsymbol{U}}\cdot(\Delta\boldsymbol{u}\langle P\rangle)+\frac{1}{\tau_v}\boldsymbol{\nabla}_{\boldsymbol{V}}\cdot(\boldsymbol{u}_{cm}\langle P\rangle)\right].\end{aligned} \tag{2.9}$$

Subtracting (2.7) from (2.9), and making terms dimensionless with the integral length scale (L), integral time scale (τ_I), and isotropic turbulence r.m.s. fluctuating velocity (u_{rms}), yields:

$$\begin{aligned}&\frac{\partial P'}{\partial t}+\boldsymbol{\nabla}_{\boldsymbol{r}}\cdot(\boldsymbol{U}P')+\boldsymbol{\nabla}_{\boldsymbol{x}}\cdot(\boldsymbol{V}P')-\frac{1}{St_I}\boldsymbol{\nabla}_{\boldsymbol{U}}\cdot(\boldsymbol{U}P')-\frac{1}{St_I}\boldsymbol{\nabla}_{\boldsymbol{V}}\cdot(\boldsymbol{V}P')\\&\quad+\frac{1}{St_I}\boldsymbol{\nabla}_{\boldsymbol{U}}\cdot(\Delta\boldsymbol{u}P')+\frac{1}{St_I}\boldsymbol{\nabla}_{\boldsymbol{V}}\cdot(\boldsymbol{u}_{cm}P')\\&=-\frac{1}{St_I}\boldsymbol{\nabla}_{\boldsymbol{U}}\cdot(\Delta\boldsymbol{u}\langle P\rangle)-\frac{1}{St_I}\boldsymbol{\nabla}_{\boldsymbol{V}}\cdot(\boldsymbol{u}_{cm}\langle P\rangle)+\frac{1}{St_I}\boldsymbol{\nabla}_{\boldsymbol{U}}\cdot\langle\Delta\boldsymbol{u}P'\rangle+\frac{1}{St_I}\boldsymbol{\nabla}_{\boldsymbol{V}}\cdot\langle\boldsymbol{u}_{cm}P'\rangle.\end{aligned} \tag{2.10}$$

Since $\langle P\rangle$ accounts for averaging over fluid time scales, but particles relax over longer time scales $\sim\tau_v$, one can expect a perturbation of P with respect to $\langle P\rangle$. We can write P as a perturbation expansion in terms of $1/St_I$,

$$P=P_0+\frac{1}{St_I}P_1+O\left(\frac{1}{St_I^2}\right), \tag{2.11}$$

where $St_I = \tau_v/\tau_I$ is the particle Stokes number defined with respect to the turbulence integral time scale τ_I. Comparing $P = \langle P\rangle + P'$ with (2.11), we can see that $\langle P\rangle = P_0$, and that to leading order $P' \sim (1/St)P_1$. We can now see from (2.10) that the last four terms on the left-hand side and the last two terms on the right-hand side are $O(1/St_I^2)$, while the remaining terms are all $O(1/St_I)$.

Considering the $O(1/St_I)$ terms in (2.10), we get:

$$\frac{\partial P_1}{\partial t} + \nabla_{\boldsymbol{r}} \cdot (\boldsymbol{U}P_1) + \nabla_{\boldsymbol{x}} \cdot (\boldsymbol{V}P_1) = -\nabla_{\boldsymbol{U}} \cdot (\Delta \boldsymbol{u}\langle P\rangle) - \nabla_{\boldsymbol{V}} \cdot (\boldsymbol{u}_{cm}\langle P\rangle). \tag{2.12}$$

Equation (2.12) is a Lagrangian evolution equation of P_1 in the $(\boldsymbol{r}, \boldsymbol{x}, t)$ space, with $\boldsymbol{U}$ and $\boldsymbol{V}$ held fixed; (2.12) may then be written as:

$$\left.\frac{\mathrm{d}P_1}{\mathrm{d}t}\right|_{\boldsymbol{U},\boldsymbol{V}} = -\nabla_{\boldsymbol{U}} \cdot (\Delta \boldsymbol{u}\langle P\rangle) - \nabla_{\boldsymbol{V}} \cdot (\boldsymbol{u}_{cm}\langle P\rangle). \tag{2.13}$$

From (2.13), we can write:

$$\begin{aligned} P_1 \;=\; & -\int_{-\infty}^{s} \mathrm{d}t' \left\{ \nabla_{\boldsymbol{U}} \cdot \left[\Delta \boldsymbol{u}\left(\boldsymbol{r}(t'), \boldsymbol{x}(t'), t'\right) \langle P\rangle(\boldsymbol{r}', \boldsymbol{U}, \boldsymbol{x}', \boldsymbol{V}; t') \right] \right. \\ & \left. + \; \nabla_{\boldsymbol{V}} \cdot \left[\boldsymbol{u}_{cm}\left(\boldsymbol{R}_1(t'), \boldsymbol{R}_2(t'), t'\right) \langle P\rangle(\boldsymbol{r}', \boldsymbol{U}, \boldsymbol{x}', \boldsymbol{V}; t') \right] \right\} \\ =\; & -\int_{-\infty}^{s} \mathrm{d}t' \left\{ \Delta \boldsymbol{u}\left(\boldsymbol{r}(t'), \boldsymbol{x}(t'), t'\right) \cdot \nabla_{\boldsymbol{U}} \langle P\rangle(t') + \boldsymbol{u}_{cm}\left(\boldsymbol{R}_1(t'), \boldsymbol{R}_2(t'), t'\right) \cdot \nabla_{\boldsymbol{V}} \langle P\rangle(t') \right\} \end{aligned} \tag{2.14}$$

where $\boldsymbol{r}' = \boldsymbol{r}(t')$, $\boldsymbol{x}' = \boldsymbol{x}(t')$, and s is a characteristic variable along the Lagrangian trajectory such that $\mathrm{d}t/\mathrm{d}s = 1$, and $(\mathrm{d}\boldsymbol{x}'/\mathrm{d}t')|_{t'=s} = \boldsymbol{V}$ and $(\mathrm{d}\boldsymbol{r}'/\mathrm{d}t')|_{t'=s} = \boldsymbol{U}$. At the upper integration limit s, we have $\boldsymbol{r}(s) = \boldsymbol{r}(t) = \boldsymbol{r}$. We have also used the shorthand notation $\langle P\rangle(t') = \langle P\rangle(\boldsymbol{r}', \boldsymbol{U}, \boldsymbol{x}', \boldsymbol{V}; t')$. The integral in (2.14) can be reduced to a time integral at fixed positions if the two convective terms on the left-hand side of (2.12) can be neglected compared to $\partial P_1/\partial t$, which would yield:

$$\begin{aligned} \langle \Delta \boldsymbol{u} P'\rangle \;=\; & -\frac{1}{St_I^2}\int_{-\infty}^{t} \mathrm{d}t' \left\{ \left\langle \Delta \boldsymbol{u}(\boldsymbol{r}, \boldsymbol{x}, t) \Delta \boldsymbol{u}(\boldsymbol{r}, \boldsymbol{x}, t') \right\rangle \cdot \nabla_{\boldsymbol{U}} \langle P\rangle(t') \right. \\ & \left. + \left\langle \Delta \boldsymbol{u}(\boldsymbol{r}, \boldsymbol{x}, t) \boldsymbol{u}_{cm}(\boldsymbol{R}_1(t), \boldsymbol{R}_2(t), t') \right\rangle \cdot \nabla_{\boldsymbol{V}} \langle P\rangle(t') \right\}, \end{aligned} \tag{2.15}$$

$$\begin{aligned} \langle \boldsymbol{u}_{cm} P'\rangle \;=\; & -\frac{1}{St_I^2}\int_{-\infty}^{t} \mathrm{d}t' \left\{ \left\langle \boldsymbol{u}_{cm}(\boldsymbol{R}_1(t), \boldsymbol{R}_2(t), t) \Delta \boldsymbol{u}(\boldsymbol{r}, \boldsymbol{x}, t') \right\rangle \cdot \nabla_{\boldsymbol{U}} \langle P\rangle(t') \right. \\ & \left. + \left\langle \boldsymbol{u}_{cm}(\boldsymbol{R}_1(t), \boldsymbol{R}_2(t), t) \boldsymbol{u}_{cm}(\boldsymbol{R}_1(t), \boldsymbol{R}_2(t), t') \right\rangle \cdot \nabla_{\boldsymbol{V}} \langle P\rangle(t') \right\}. \end{aligned} \tag{2.16}$$

In (2.15) and (2.16), $\boldsymbol{r}$ and $\boldsymbol{x}$ are essentially constant during flow time scales. The conditions under which the two convective terms on the left-hand side of (2.12) can be neglected are derived after (2.22) below. In (2.15) and (2.16), the PDF $\langle P\rangle$ is evaluated at time t'. The two-time fluid velocity correlations in (2.15) and (2.16) are significant only in the time interval $t - t'$ for which the fluid eddies are correlated. Therefore, we can write $\langle P\rangle(t') \approx \langle P\rangle(t)$, since the time scales over which $\langle P\rangle$ changes are much greater than the fluid correlation time scales. Pulling $\langle P\rangle$ out of the time integrals, and substituting (2.15) and (2.16) into the dimensionless form of (2.7), the Fokker–Planck

equation can be written as:

$$\frac{\partial\langle P\rangle}{\partial t}+\nabla_{\boldsymbol{r}}\cdot(\boldsymbol{U}\langle P\rangle)+\nabla_{\boldsymbol{x}}\cdot(\boldsymbol{V}\langle P\rangle)-\frac{1}{St_I}\nabla_{\boldsymbol{U}}\cdot(\boldsymbol{U}\langle P\rangle)-\frac{1}{St_I}\nabla_{\boldsymbol{V}}\cdot(\boldsymbol{V}\langle P\rangle)$$
$$-\nabla_{\boldsymbol{U}}\cdot(\boldsymbol{D}_{UU}\cdot\nabla_{\boldsymbol{U}}\langle P\rangle+\boldsymbol{D}_{UV}\cdot\nabla_{\boldsymbol{V}}\langle P\rangle)-\nabla_{\boldsymbol{V}}\cdot(\boldsymbol{D}_{VU}\cdot\nabla_{\boldsymbol{U}}\langle P\rangle+\boldsymbol{D}_{VV}\cdot\nabla_{\boldsymbol{V}}\langle P\rangle)=0, \tag{2.17}$$

where

$$\boldsymbol{D}_{UU}=\frac{1}{St_I^2}\widetilde{\boldsymbol{D}}_{UU}=\frac{1}{St_I^2}\int_{-\infty}^{t}\mathrm{d}t'\left\langle\Delta\boldsymbol{u}(\boldsymbol{r},\boldsymbol{x},t)\Delta\boldsymbol{u}(\boldsymbol{r},\boldsymbol{x},t')\right\rangle, \tag{2.18}$$

$$\boldsymbol{D}_{UV}=\frac{1}{St_I^2}\widetilde{\boldsymbol{D}}_{UV}=\frac{1}{St_I^2}\int_{-\infty}^{t}\mathrm{d}t'\left\langle\Delta\boldsymbol{u}(\boldsymbol{r},\boldsymbol{x},t)\boldsymbol{u}_{cm}(\boldsymbol{R}_1(t),\boldsymbol{R}_2(t),t')\right\rangle, \tag{2.19}$$

$$\boldsymbol{D}_{VU}=\frac{1}{St_I^2}\widetilde{\boldsymbol{D}}_{VU}=\frac{1}{St_I^2}\int_{-\infty}^{t}\mathrm{d}t'\left\langle\boldsymbol{u}_{cm}(\boldsymbol{R}_1(t),\boldsymbol{R}_2(t),t)\Delta\boldsymbol{u}(\boldsymbol{r},\boldsymbol{x},t')\right\rangle, \tag{2.20}$$

$$\boldsymbol{D}_{VV}=\frac{1}{St_I^2}\widetilde{\boldsymbol{D}}_{VV}=\frac{1}{St_I^2}\int_{-\infty}^{t}\mathrm{d}t'\left\langle\boldsymbol{u}_{cm}(\boldsymbol{R}_1(t),\boldsymbol{R}_2(t),t)\boldsymbol{u}_{cm}(\boldsymbol{R}_1(t),\boldsymbol{R}_2(t),t')\right\rangle. \tag{2.21}$$

In (2.18)–(2.21), $\boldsymbol{D}_{UU}$ and $\boldsymbol{D}_{VV}$ are the diffusion coefficient tensors in the $\boldsymbol{U}$-space and $\boldsymbol{V}$-space, respectively; $\boldsymbol{D}_{UV}$ and $\boldsymbol{D}_{VU}$ are the cross-diffusion coefficient tensors in the mixed $\boldsymbol{UV}$- and $\boldsymbol{VU}$-spaces, respectively. These diffusion tensors (particularly $\boldsymbol{D}_{VV}$) are analogous to the formulation of Reeks (1991), who showed that the single-particle diffusion tensor contains Lagrangian correlations of fluid velocities 'seen'. Subsequently, Minier & Peirano (2001) demonstrated that the diffusion coefficient of the slow variable may be expressed as a time integral of the temporal correlation of the fast variable, which is indeed what we observe in (2.18)–(2.21) as well. The diffusion coefficient tensors can also be interpreted as the time integrals of the two-time correlations of the accelerations of the pair relative and/or centre-of-mass velocities caused by fluid velocity fluctuations. For example,

$$\boldsymbol{D}_{UU}=\int_{-\infty}^{t}\left\langle\dot{\boldsymbol{U}}(t)\dot{\boldsymbol{U}}(t')\right\rangle\mathrm{d}t' \tag{2.22}$$

where $\dot{\boldsymbol{U}}(t)=(1/St_I)\Delta\boldsymbol{u}(t)+O(1/St_I^2)$.

We will now derive, using an order-of-magnitude analysis, the conditions to be satisfied for neglecting the two convective terms in (2.12) so that the fluid velocity correlations seen by the particles can be approximated as those at fixed positions in space. The neglect of $\nabla_{\boldsymbol{x}}\cdot(\boldsymbol{V}P')$ compared with $\partial P'/\partial t$ requires that the change in the position of the pair centre of mass during the integral-scale fluid correlation time be small compared with the integral length scale, i.e. $\langle V^2\rangle^{1/2}\ll 1$. Since it is well known that $\langle V^2\rangle\sim O(1/St_I)$ (Reeks 1991), this condition is satisfied for $St_I\gg 1$.

Neglecting $\nabla_{\boldsymbol{r}}\cdot(\boldsymbol{U}P')$ compared to $\partial P'/\partial t$ requires the change in pair separation (r) during the fluid correlation time τ_r of an eddy of size r to be small compared with the eddy size, i.e. $U\tau_r\ll r$. While this condition is not satisfied for all particle pairs, we will see that it is satisfied for those pairs that are significantly influenced by the fluid eddies of size r.

The relative-velocity PDFs from Sundaram & Collins (1997) indicate that at separations smaller than the integral length scale ($r/L<1$) the high-inertia ($St_\eta>1$)

particle pairs can be divided into two broad classes: 'lingerers' and 'flyers'. Lingerers are low-relative-velocity pairs that are highly correlated and remain correlated far longer than the time scales of fluid that influence their relative motion. Flyers are uncorrelated pairs with large relative velocities, whose relative motion is unaffected by the fluid eddies with length scales comparable with their separation. For a flyer pair with separation r, the change in relative velocity ΔU due to their interaction with a fluid eddy of size r is small compared with the pair relative velocity, i.e. $\Delta U \ll U$. For lingerers, $\Delta U \sim U$.

The change in the relative velocity of a pair while they interact at separation r is given by the square root of the velocity-space diffusivity times their interaction time, i.e. $\Delta U \sim (\boldsymbol{D}_{UU}\tau_r)^{1/2}$, where τ_r is the time scale of the fluid eddy of size r. For a 'lingerer' pair, using $\Delta U \sim U$, we find that such pairs have a relative velocity $U \sim (\boldsymbol{D}_{UU}r)^{1/3}$. In dimensional form, the relative-velocity-space diffusion coefficient is the product of the square of the acceleration due to the eddy $(u_{eddy}/\tau_v)^2$ and the correlation time of the eddy τ_r. Since $u_{eddy} \sim r/\tau_r$, $\boldsymbol{D}_{UU} \sim r^2/(\tau_v^2\tau_r)$. Thus, the relative velocity for the lingerers is $U \sim r/(\tau_r\tau_v^2)^{1/3}$, and the change of the relative position during the fluid time scale is $U\tau_r = rSt_r^{-2/3}$, where $St_r = \tau_v/\tau_r$ is the Stokes number defined based on the eddies of size r. We see then that the convective term in $\boldsymbol{r}$-space on the left-hand side of (2.12) can be neglected as long as the Stokes number based on eddies of size r is large, i.e. $St_r = \tau_v/\tau_r \gg 1$.

In the previous discussion, we derived a conservation equation for the high-dimensional PDF, $\langle P\rangle(\boldsymbol{r}, \boldsymbol{U}, \boldsymbol{x}, \boldsymbol{V}; t)$. The dependence of $\langle P\rangle$ on $\boldsymbol{x}$ can be dropped owing to the spatial homogeneity of the flow. Since we are primarily interested in the statistics of the pair relative velocity and relative position, we will consider a more convenient, lower-dimensional PDF defined as: $\Omega(\boldsymbol{r}, \boldsymbol{U}) = \int\langle P\rangle(\boldsymbol{r}, \boldsymbol{U}, \boldsymbol{V}; t)\,\mathrm{d}\boldsymbol{V}$. (The effects of $\boldsymbol{x}$ and $\boldsymbol{V}$ are included in the diffusion coefficient closure.)

Integrating (2.17) over the $\boldsymbol{V}$-space, we get:

$$\frac{\partial\Omega}{\partial t} + \boldsymbol{\nabla}_{\boldsymbol{r}}\cdot(\boldsymbol{U}\Omega) - \frac{1}{St_I}\boldsymbol{\nabla}_{\boldsymbol{U}}\cdot(\boldsymbol{U}\Omega) - \frac{1}{St^2}\boldsymbol{\nabla}_{\boldsymbol{U}}\cdot(\widetilde{\boldsymbol{D}}_{UU}\cdot\boldsymbol{\nabla}_{\boldsymbol{U}}\Omega) = 0. \tag{2.23}$$

As discussed in Reeks (1991) and Minier & Peirano (2001), the Fokker–Planck equation governing the PDF $\Omega(\boldsymbol{r}, \boldsymbol{U})$ is a consequence of the Stokes numbers of interest, $St_r \gg 1$. For these Stokes numbers, one may represent the effects of the underlying turbulence on the relative velocity $\boldsymbol{U}$ as a white-noise term that is manifested as a phase-space diffusion tensor $\boldsymbol{D}_{UU}$.

In arriving at (2.23), we have used the divergence theorem in the centre-of-mass velocity space:

$$\begin{aligned}\int_{\boldsymbol{V}} \boldsymbol{\nabla}_{\boldsymbol{V}}\cdot(\widetilde{\boldsymbol{D}}_{VU}\cdot\boldsymbol{\nabla}_{\boldsymbol{U}}\langle P\rangle + \widetilde{\boldsymbol{D}}_{VV}\cdot\boldsymbol{\nabla}_{\boldsymbol{V}}\langle P\rangle)\mathrm{d}\boldsymbol{V}\\ = \int_{\partial\boldsymbol{V}}(\widetilde{\boldsymbol{D}}_{VU}\cdot\boldsymbol{\nabla}_{\boldsymbol{U}}\langle P\rangle + \widetilde{\boldsymbol{D}}_{VV}\cdot\boldsymbol{\nabla}_{\boldsymbol{V}}\langle P\rangle)\cdot\boldsymbol{n}\,\mathrm{d}S_{\boldsymbol{V}} = 0\end{aligned} \tag{2.24}$$

where $\int_{\partial\boldsymbol{V}}$ represents integration over a boundary in the $\boldsymbol{V}$-space, and $\boldsymbol{n}$ is the normal to this boundary. We take the boundary to be at a large velocity so that $|\boldsymbol{V}| \gg \langle V^2\rangle^{1/2}$, thereby $\langle P\rangle$ is essentially zero on the boundary. Hence, the integration $\int_{\partial\boldsymbol{V}}$ is zero. Also, note that

$$\begin{aligned}\boldsymbol{\nabla}_{\boldsymbol{U}}\cdot(\widetilde{\boldsymbol{D}}_{UV}\cdot\boldsymbol{\nabla}_{\boldsymbol{V}}\langle P\rangle) &= \boldsymbol{\nabla}_{\boldsymbol{U}}\cdot[\boldsymbol{\nabla}_{\boldsymbol{V}}\cdot(\widetilde{\boldsymbol{D}}_{UV}\langle P\rangle) - \langle P\rangle\boldsymbol{\nabla}_{\boldsymbol{V}}\cdot\widetilde{\boldsymbol{D}}_{UV}]\\ &= \boldsymbol{\nabla}_{\boldsymbol{V}}\cdot[\boldsymbol{\nabla}_{\boldsymbol{U}}\cdot(\widetilde{\boldsymbol{D}}_{UV}\langle P\rangle)].\end{aligned} \tag{2.25}$$

Hence, this term also vanishes when integrated over the $\boldsymbol{V}$-space, where we have used $\boldsymbol{\nabla}_{\boldsymbol{V}} \cdot \widetilde{\boldsymbol{D}}_{UV} = 0$, as $\widetilde{\boldsymbol{D}}_{UV}$ is not a function of $\boldsymbol{V}$.

Equation (2.23) is similar to (34) in Zaichik & Alipchenkov (2003). However, as discussed in § 1, their formulation consists of two diffusion terms, one of which is the same as $\boldsymbol{D}_{UU}$ in the limit of $St_I \gg 1$. The next part of our theory deals with the derivation of an analytical formulation for predicting $\boldsymbol{D}_{UU}$.

2.3. *Derivation of diffusion coefficient tensor in the pair-relative-velocity space*

We have already seen that the diffusion coefficient tensor $\boldsymbol{D}_{UU}$ can be written as:

$$\begin{aligned}\boldsymbol{D}_{UU} &= \frac{1}{St_I^2}\widetilde{\boldsymbol{D}}_{UU} \\ &= \frac{1}{St_I^2}\int_{-\infty}^{t} \left\langle \Delta\boldsymbol{u}(\boldsymbol{r},\boldsymbol{x},t)\Delta\boldsymbol{u}(\boldsymbol{r},\boldsymbol{x},t')\right\rangle \mathrm{d}t' \\ &= \frac{1}{St_I^2}\int_{-\infty}^{0} \langle \Delta\boldsymbol{u}(\boldsymbol{r},\boldsymbol{x},0)\Delta\boldsymbol{u}(\boldsymbol{r},\boldsymbol{x},t)\rangle \,\mathrm{d}t \end{aligned} \tag{2.26}$$

where $\Delta\boldsymbol{u}(\boldsymbol{r},\boldsymbol{x},t) = \boldsymbol{u}[\boldsymbol{x}+\frac{1}{2}\boldsymbol{r},t] - \boldsymbol{u}[\boldsymbol{x}-\frac{1}{2}\boldsymbol{r},t]$, and $\boldsymbol{x}+\frac{1}{2}\boldsymbol{r}$ and $\boldsymbol{x}-\frac{1}{2}\boldsymbol{r}$ represent the positions of a pair of particles with separation $\boldsymbol{r}$.

The Eulerian two-time fluid velocity correlations contained in $\langle\Delta\boldsymbol{u}(\boldsymbol{r},\boldsymbol{x},0)\Delta\boldsymbol{u}(\boldsymbol{r},\boldsymbol{x},t)\rangle$ can be evaluated using DNS. The objective of this study, however, is to derive an analytical, closed-form expression for $\boldsymbol{D}_{UU}$. To this end, the process of converting the two-time correlations into two-point spatial correlations is discussed next.

Recall that, in arriving at (2.26), we have assumed that $St_I \gg 1$ and $St_r \gg 1$. With these assumptions, the particles are nearly stationary so that the temporal evolution of the relative velocity of a particle pair is controlled primarily by the evolution of the fluid velocity field at the particle positions. Moreover, the temporal change in $\Delta\boldsymbol{u}$ experienced by the particle pair is primarily due to the evolution of the turbulence scales and not due to pair motion itself. We will represent the temporal evolution of $\Delta\boldsymbol{u}$ at two positions separated by $\boldsymbol{r}$ based on an approximation in which a frozen turbulent velocity field associated with the eddies of size r is advected by larger, integral-scale eddies. Hence, one may replace the above Eulerian two-time correlation by a two-point spatial correlation between two pairs with the same $\boldsymbol{r}$, but with the centres of mass separated by $\boldsymbol{u}_I t$, where $\boldsymbol{u}_I$ is the large-scale velocity. This would give us:

$$\boldsymbol{D}_{UU} = \frac{1}{St_I^2}\int_{-\infty}^{0} \langle \Delta\boldsymbol{u}(\boldsymbol{r},\boldsymbol{x},t)\Delta\boldsymbol{u}(\boldsymbol{r},\boldsymbol{x}+\boldsymbol{u}_I t,t)\rangle \,\mathrm{d}t. \tag{2.27}$$

In writing (2.27) from (2.26), it is assumed that the large-scale velocity $\boldsymbol{u}_I$ remains essentially constant during $[t, 0]$. This is reasonable because $\boldsymbol{u}_I$ does not evolve significantly during the time τ_r of interaction between an eddy of size r and a pair at separation r, as the turnover time τ_r of eddies of size r is much smaller than the turnover time of large-scale eddies. Though this approach is similar to Taylor's frozen-turbulence hypothesis, the principal difference is that in Taylor's hypothesis, frozen turbulence is advected by the mean flow, whereas in the current approach, eddies of size r (r is the pair separation) are advected by the integral-scale eddies.

One may relax the requirement of $St_I \gg 1$ so that for particles with $St_I \lesssim 1$, the pair centre of mass is not stationary. When $St_r \gg 1$ and $St_I \lesssim 1$, the difference is that while

the separation $\boldsymbol{r}$ does not change significantly, the centre-of-mass position may change due to interactions with eddies of time scales $\sim\tau_v$, the centre-of-mass response time. Therefore, one will have to account for the relative motion between the large-scale eddies that are passively advecting eddies of size r and the centre-of-mass position. This is done by replacing $\boldsymbol{u}_I$ with the relative velocity $\boldsymbol{W}$. This change makes the theory applicable for large-inertia particles that satisfy $St_r \gg 1$ and not necessarily $St_I \gg 1$. Since $\boldsymbol{W}$ is principally influenced by the large-scale fluid eddies, its PDF $\Phi(\boldsymbol{W})$, can be considered Gaussian (Batchelor 1953):

$$\Phi(\boldsymbol{W}) = \frac{1}{\sqrt{\left(2\pi W_{rms}^2\right)^3}} \mathrm{e}^{-W^2/(2W_{rms}^2)} \tag{2.28}$$

where W_{rms} is the r.m.s. fluctuating velocity of $\boldsymbol{W}$ and needs to be determined. The diffusivity can then be expressed as an average over all values of the large-scale velocity $\boldsymbol{W}$ as:

$$\boldsymbol{D}_{UU}(\boldsymbol{r}) = \int \widehat{\boldsymbol{D}}_{UU}(\boldsymbol{r}, W)\Phi(\boldsymbol{W})\,\mathrm{d}\boldsymbol{W} \tag{2.29}$$

where

$$\begin{aligned}
\widehat{\boldsymbol{D}}_{UU} &= \frac{1}{St_I^2}\int_{-\infty}^{0} \langle \Delta\boldsymbol{u}(\boldsymbol{r}, \boldsymbol{x}, t)\Delta\boldsymbol{u}(\boldsymbol{r}, \boldsymbol{x}+\boldsymbol{W}t, t)\rangle\,\mathrm{d}t \\
&= \frac{1}{St_I^2}\int_{-\infty}^{0} \Big\langle \left[\boldsymbol{u}\left(\boldsymbol{x}+\frac{1}{2}\boldsymbol{r}, t\right) - \boldsymbol{u}\left(\boldsymbol{x}-\frac{1}{2}\boldsymbol{r}, t\right)\right] \\
&\quad \times \left[\boldsymbol{u}\left(\boldsymbol{x}+\boldsymbol{W}t+\frac{1}{2}\boldsymbol{r}, t\right) - \boldsymbol{u}\left(\boldsymbol{x}+\boldsymbol{W}t-\frac{1}{2}\boldsymbol{r}, t\right)\right]\Big\rangle\,\mathrm{d}t \\
&= \frac{1}{St_I^2}\int_{-\infty}^{0} \Big\langle \boldsymbol{u}\left(\boldsymbol{x}+\frac{1}{2}\boldsymbol{r}, t\right)\boldsymbol{u}\left(\boldsymbol{x}+\boldsymbol{W}t+\frac{1}{2}\boldsymbol{r}, t\right) \\
&\quad - \boldsymbol{u}\left(\boldsymbol{x}+\frac{1}{2}\boldsymbol{r}, t\right)\boldsymbol{u}\left(\boldsymbol{x}+\boldsymbol{W}t-\frac{1}{2}\boldsymbol{r}, t\right) \\
&\quad - \boldsymbol{u}\left(\boldsymbol{x}-\frac{1}{2}\boldsymbol{r}, t\right)\boldsymbol{u}\left(\boldsymbol{x}+\boldsymbol{W}t+\frac{1}{2}\boldsymbol{r}, t\right) \\
&\quad + \boldsymbol{u}\left(\boldsymbol{x}-\frac{1}{2}\boldsymbol{r}, t\right)\boldsymbol{u}\left(\boldsymbol{x}+\boldsymbol{W}t-\frac{1}{2}\boldsymbol{r}, t\right)\Big\rangle\,\mathrm{d}t.
\end{aligned} \tag{2.30}$$

In (2.30), there are four Eulerian two-point velocity correlation terms. Writing the two-point velocity correlation tensors in terms of the velocity spectrum tensor, $\boldsymbol{R}(\boldsymbol{k})$, we get:

$$\widehat{\boldsymbol{D}}_{UU} = \frac{1}{St_I^2}\int \boldsymbol{R}(\boldsymbol{k})\left(2 - \mathrm{e}^{-\mathrm{i}\boldsymbol{k}\cdot\boldsymbol{r}} - \mathrm{e}^{\mathrm{i}\boldsymbol{k}\cdot\boldsymbol{r}}\right)\mathrm{d}\boldsymbol{k}\int_{-\infty}^{0}\mathrm{e}^{\mathrm{i}\boldsymbol{k}\cdot\boldsymbol{W}t}\mathrm{d}t \tag{2.31}$$

where $\boldsymbol{k}$ is the wavenumber vector. The second (time) integral in (2.31) can be conveniently evaluated using the standard Fourier transforms, giving us:

$$\widehat{\boldsymbol{D}}_{UU} = \frac{1}{St_I^2}\int \boldsymbol{R}(\boldsymbol{k})\left[1 - \cos(\boldsymbol{k}\cdot\boldsymbol{r})\right]\delta\left(\frac{\boldsymbol{k}\cdot\boldsymbol{W}}{2\pi}\right)\mathrm{d}\boldsymbol{k}. \tag{2.32}$$

Note that $\delta((\boldsymbol{k}\cdot\boldsymbol{W})/2\pi)$ is non-zero only when $\boldsymbol{k}\cdot\boldsymbol{W}=0$, i.e. when $\boldsymbol{k}\perp\boldsymbol{W}$. Let $\boldsymbol{\xi}=(\xi,\phi)$ represent, in polar coordinates, the plane perpendicular to $\boldsymbol{W}$. We can now write:

$$\mathrm{d}\boldsymbol{k}=\frac{1}{W}\xi\,\mathrm{d}\xi\,\mathrm{d}\phi\,\mathrm{d}(\boldsymbol{k}\cdot\boldsymbol{W}) \tag{2.33}$$

where $W=|\boldsymbol{W}|$. This gives us:

$$\widehat{\boldsymbol{D}}_{UU}(\boldsymbol{r},W)=\frac{2\pi}{St_I^2}\frac{1}{W}\int_0^\infty\xi\,\mathrm{d}\xi\int_0^{2\pi}\frac{E(\xi)}{4\pi\xi^2}\left(\delta_{ij}-\frac{\xi_i\xi_j}{\xi^2}\right)[1-\cos(\xi\rho\cos\phi)]\,\mathrm{d}\phi \tag{2.34}$$

where $\boldsymbol{\rho}$ is the projection of $\boldsymbol{r}$ into the $\boldsymbol{\xi}$-plane, $\rho=|\boldsymbol{\rho}|$, and we have written $R(\xi)$ in terms of the energy spectrum $E(\xi)$.

For isotropic turbulence, we can write $\widehat{\boldsymbol{D}}_{UU}$ as:

$$\widehat{D}_{UU,ij}=\widehat{D}_{UU,\perp}\left(\delta_{ij}-\frac{r_ir_j}{r^2}\right)+\widehat{D}_{UU,\parallel}\frac{r_ir_j}{r^2}. \tag{2.35}$$

Using (2.34), we will develop expressions for $\widehat{D}_{UU,\perp}$ and $\widehat{D}_{UU,\parallel}$.

2.3.1. *Derivation of $\widehat{D}_{UU,\perp}$ and $\widehat{D}_{UU,\parallel}$*

The procedure to derive the expressions for $\widehat{D}_{UU,\perp}$ and $\widehat{D}_{UU,\parallel}$ is quite involved, and only the main steps are presented here. Since $\boldsymbol{\rho}$ is the projection of $\boldsymbol{r}$ into the $\boldsymbol{\xi}$-plane, we can write:

$$\rho_i=\left(\delta_{ij}-\frac{W_iW_j}{W^2}\right)r_j, \tag{2.36}$$

$$\cos\phi=\frac{\rho_i\xi_i}{\rho\xi}=\frac{r_i\xi_i}{r\xi}. \tag{2.37}$$

It can be shown that $\widehat{D}_{UU,ij}$ can be expressed as follows:

$$\widehat{D}_{UU,ij}=\frac{2\pi}{St_I^2}\frac{1}{W}\left[A\left(\frac{W_iW_j}{W^2}+\frac{\rho_i\rho_j}{\rho^2}\right)+D\left(\delta_{ij}-\frac{W_iW_j}{W^2}-2\frac{\rho_i\rho_j}{\rho^2}\right)\right] \tag{2.38}$$

where

$$A=\int_0^\infty\xi\,\mathrm{d}\xi\int_0^{2\pi}\frac{E(\xi)}{4\pi\xi^2}[1-\cos(\xi\rho\cos\phi)]\,\mathrm{d}\phi, \tag{2.39}$$

$$D=\int_0^\infty\xi\,\mathrm{d}\xi\int_0^{2\pi}\frac{E(\xi)}{4\pi\xi^2}[1-\cos(\xi\rho\cos\phi)]\cos^2\phi\,\mathrm{d}\phi. \tag{2.40}$$

Using (2.35) and (2.38), we can derive expressions for $\widehat{D}_{UU,\perp}$ and $\widehat{D}_{UU,\parallel}$:

$$\begin{aligned}\widehat{D}_{UU,\perp}&=\frac{1}{2}\widehat{D}_{UU,ij}\left(\delta_{ij}-\frac{\rho_i\rho_j}{\rho^2}\right)\\&=\frac{1}{2}\frac{2\pi}{St_I^2}\frac{1}{W}\left(A+D\sin^2\theta\right)\end{aligned} \tag{2.41}$$

and

$$\widehat{D}_{UU,\parallel} = \widehat{D}_{UU,ij}\frac{\rho_i\rho_j}{\rho^2} = \frac{2\pi}{St_I^2}\frac{1}{W}\left(A - D\sin^2\theta\right) \tag{2.42}$$

where

$$\sin^2\theta = \frac{\rho_i\rho_j}{\rho^2}\frac{r_i r_j}{r^2}, \quad \cos^2\theta = \frac{W_i W_j}{W^2}\frac{r_i r_j}{r^2}. \tag{2.43a,b}$$

We can now eliminate the dependence on W in (2.34) using (2.29). For isotropic turbulence, we write $\boldsymbol{D}_{UU}(\boldsymbol{r})$ as:

$$D_{UU,ij}(r) = D_{UU,\perp}(r)\left(\delta_{ij} - \frac{r_i r_j}{r^2}\right) + D_{UU,\parallel}(r)\frac{r_i r_j}{r^2} \tag{2.44}$$

where

$$D_{UU,\perp} = \frac{1}{2}\frac{2\pi}{St_I^2}\int\frac{1}{W}\left(A + D\sin^2\theta\right)\Phi(\boldsymbol{W})\,\mathrm{d}\boldsymbol{W}, \tag{2.45}$$

$$D_{UU,\parallel} = \frac{2\pi}{St_I^2}\int\frac{1}{W}\left(A - D\sin^2\theta\right)\Phi(\boldsymbol{W})\,\mathrm{d}\boldsymbol{W}. \tag{2.46}$$

Using the expressions for A and D from (2.39) and (2.40), respectively, we get:

$$D_{UU,\perp}(r) = \frac{1}{2}\frac{2\pi}{St_I^2}\int\frac{1}{W}\Phi(\boldsymbol{W})\,\mathrm{d}\boldsymbol{W}\int_0^\infty \xi\,\mathrm{d}\xi\int_0^{2\pi}\frac{E(\xi)}{4\pi\xi^2} \times\left[1-\cos(\xi\rho\cos\phi)\right]\left(1+\cos^2\phi\sin^2\theta\right)\mathrm{d}\phi, \tag{2.47}$$

$$D_{UU,\parallel}(r) = \frac{2\pi}{St_I^2}\int\frac{1}{W}\Phi(\boldsymbol{W})\,\mathrm{d}\boldsymbol{W}\int_0^\infty \xi\,\mathrm{d}\xi\int_0^{2\pi}\frac{E(\xi)}{4\pi\xi^2} \times\left[1-\cos(\xi\rho\cos\phi)\right]\left(1-\cos^2\phi\sin^2\theta\right)\mathrm{d}\phi \tag{2.48}$$

where $\mathrm{d}\boldsymbol{W} = W^2\sin\theta\,\mathrm{d}\theta\,\mathrm{d}\psi\,\mathrm{d}W$; $\psi\in[0,2\pi]$ is the azimuthal angle.

After integrating over $\boldsymbol{W}$-space and over ϕ, (2.47) and (2.48) can be simplified substantially, giving us:

$$D_{UU,\perp}(r) = \frac{1}{2}\frac{2\pi^2}{St_I^2}\sqrt{\frac{1}{(2\pi)^3 W_{rms}^2}} \times\int_0^\infty\frac{E(\xi)}{\xi}\left[\frac{8}{3} - \frac{4\sin(r\xi)}{r\xi} - \frac{4\cos(r\xi)}{r^2\xi^2} + \frac{4\sin(r\xi)}{r^3\xi^3}\right]\mathrm{d}\xi \tag{2.49}$$

$$D_{UU,\parallel}(r) = \frac{2\pi^2}{St_I^2}\sqrt{\frac{1}{(2\pi)^3 W_{rms}^2}}\int_0^\infty\frac{E(\xi)}{\xi}\left[\frac{4}{3} + \frac{4\cos(r\xi)}{r^2\xi^2} - \frac{4\sin(r\xi)}{r^3\xi^3}\right]\mathrm{d}\xi. \tag{2.50}$$

Equations (2.49) and (2.50) are substituted back into (2.44) to give us the averaged diffusion coefficient, $D_{UU,ij}$. To complete the closure of the diffusion-current term, however, we require an expression for W_{rms}. This is discussed next.

2.4. *Derivation of an expression for W_{rms}*

In the limit of $St_I \gg 1$, $W_{rms} \approx u_{rms}$, where u_{rms} is the Eulerian r.m.s. fluctuating velocity of isotropic turbulence. But, when $St_I \lesssim 1$, W_{rms} needs to be estimated, which is the purpose of this section. Using the definition of W_{rms}, we can write:

$$W_{rms}^2 = \tfrac{1}{3}\left\langle (u_i - V_i)^2 \right\rangle = \tfrac{1}{3}\left[\left\langle u_i^2 \right\rangle + \left\langle V_i^2 \right\rangle - 2\left\langle V_i u_i \right\rangle\right] \tag{2.51}$$

where V_i is the velocity of the pair centre of mass, u_i is the fluid velocity with which eddies of size r are advected past the pair, and $\langle u_i^2 \rangle = \langle u_1^2 + u_2^2 + u_3^2 \rangle$ ($\langle V_i^2 \rangle$ follows a similar notation).

The velocity of the pair centre of mass is governed by

$$\frac{\mathrm{d}V_i}{\mathrm{d}t} = \frac{u_{cm,i} - V_i}{\tau_v} \tag{2.52}$$

where $u_{cm,i}$ was defined in (2.5). Multiplying (2.52) with V_i and ensemble-averaging yields

$$\frac{\mathrm{d}\left\langle \frac{1}{2} V_i^2 \right\rangle}{\mathrm{d}t} = \frac{\langle u_i V_i \rangle - \langle V_i^2 \rangle}{\tau_v}. \tag{2.53}$$

We have replaced $\langle u_{cm,i} V_i \rangle$ on the right-hand side of (2.53) with $\langle u_i V_i \rangle$. While this approximation is not exact, it may be noted that both $u_i - V_i$ and $u_{cm,i} - V_i$ are determined by eddies whose sizes are of the order of or smaller than r so that these two quantities may be expected to have similar statistics.

At steady state, $\langle V_i u_i \rangle = \langle V_i^2 \rangle$. This means that from (2.52)

$$\begin{aligned} W_{rms}^2 &= \frac{1}{3}\left[\left\langle u_i^2 \right\rangle - \left\langle V_i^2 \right\rangle\right] = \frac{1}{3}\left\langle u_i^2 \right\rangle \left(1 - \frac{\left\langle V_i^2 \right\rangle}{\left\langle u_i^2 \right\rangle}\right) \\ &= u'^2 \left(1 - \frac{V'^2}{u'^2}\right) \end{aligned} \tag{2.54}$$

where $\frac{1}{3}\langle u_i^2 \rangle = u'^2$, and similarly $\frac{1}{3}\langle V_i^2 \rangle = V'^2$. Here, u'^2 is the variance of the fluid velocity seen by the centre of mass, and V'^2 is the variance of the centre-of-mass velocity. Therefore, in order to close W_{rms}, one needs expressions for u' and the ratio V'/u'.

The well-known Tchen theory (see Jung, Yeo & Lee 2008) provides the following expression for V'^2/u'^2:

$$\frac{V'^2}{u'^2} = \frac{T_L/\tau_v}{1 + T_L/\tau_v}, \tag{2.55}$$

which was later refined by Jung *et al.* (2008):

$$\frac{V'^2}{u'^2} = \frac{\tau_\eta(\tau_v + T') + \tau_v T'}{(\tau_\eta + \tau_v)(\tau_v + T')}, \tag{2.56}$$

where T_L is the fluid Lagrangian integral time scale, $T' = T_{fp} - \tau_\eta$, τ_η is the Kolmogorov time scale and T_{fp} is the Lagrangian integral time scale of fluid velocities seen by the particles:

$$T_{fp} = \frac{\displaystyle\int_0^\infty \mathrm{d}t \langle u(t_0) u(t + t_0) \rangle}{\langle u^2(t_0) \rangle} \tag{2.57}$$

where u is the fluid velocity seen by the particles, and t_0 is a reference time. Jung *et al.* (2008) provided the following expression for T_{fp}:

$$\frac{T_{fp}}{T_L} = 0.245\exp\left\{-\left[\frac{\ln(St_\eta/1.2)}{1.3}\right]^2\right\} + \frac{1+(T_E/T_L)(0.025\,St)^{1.5}}{1+(0.025\,St)^{1.5}} \tag{2.58}$$

where $St_\eta = \tau_v/\tau_\eta$. The Jung *et al.* (2008) refined theory of (2.56) showed excellent agreement with the DNS data. Hence, we will use (2.56) in the current study. Further, Jung *et al.* (2008) plot the ratio of particle to fluid dispersion coefficients as a function of St_η. From this plot, it can be inferred that for $St_\eta \gtrsim 4$, $u'^2 = u_{rms}^2$, i.e. for high-St particles the variance of the fluid velocity seen by the particles is nearly equal to the variance of the turbulent fluid velocity. Equation (2.58) together with (2.54) and (2.56) complete the closure for W_{rms}.

2.5. *Consistency check of the pair diffusion coefficient*

It is known that the pair diffusion coefficient of a particle pair at infinite separation is twice the diffusion coefficient of a single particle. The diffusion coefficient formulation derived above should also satisfy this requirement, and this is what we will establish in the following discussion.

Let $\boldsymbol{v}(t)$ and $\boldsymbol{y}(t)$ represent the velocity and position vectors of a single high-Stokes-number particle. The governing equation for $\boldsymbol{v}$ is (in dimensionless form):

$$\frac{\mathrm{d}\boldsymbol{v}}{\mathrm{d}t} = -\frac{1}{\tau_v}\left[\boldsymbol{v}(t) - \boldsymbol{u}(\boldsymbol{y}, t)\right]. \tag{2.59}$$

Using $\beta = 1/\tau_v$, and multiplying both sides of (2.59) with $\mathrm{e}^{\beta t}$ and simplifying gives us:

$$\boldsymbol{v}(t) = \beta\int_{-\infty}^{t} \mathrm{e}^{\beta(\tau-t)}\boldsymbol{u}(\boldsymbol{y}, \tau)\mathrm{d}\tau. \tag{2.60}$$

Substituting (2.60) into (2.59), we get:

$$\dot{\boldsymbol{v}}(t) = \frac{1}{\tau_v}\boldsymbol{u}(\boldsymbol{y}, t) + O\left(\frac{1}{\tau_v^2}\right). \tag{2.61}$$

The diffusion coefficient for a single particle, $\boldsymbol{D}_v$, can be defined as:

$$\begin{aligned}\boldsymbol{D}_v &= \int_{-\infty}^{t}\left\langle\dot{\boldsymbol{v}}(t)\dot{\boldsymbol{v}}(t')\right\rangle\mathrm{d}t' \\ &\approx \frac{1}{\tau_v^2}\int_{-\infty}^{t}\left\langle\boldsymbol{u}(\boldsymbol{y}, t)\boldsymbol{u}(\boldsymbol{y}, t')\right\rangle\mathrm{d}t' \\ &= \frac{1}{\tau_v^2}\int_{-\infty}^{0}\langle\boldsymbol{u}(\boldsymbol{y}, 0)\boldsymbol{u}(\boldsymbol{y}, t)\rangle\,\mathrm{d}t.\end{aligned} \tag{2.62}$$

As seen previously, we will convert the two-time, two-point Lagrangian correlation in (2.62) into a two-point Eulerian correlation:

$$\begin{aligned}\boldsymbol{D}_v &= \frac{1}{\tau_v^2}\int_{-\infty}^{0}\langle \boldsymbol{u}(\boldsymbol{y},t)\boldsymbol{u}(\boldsymbol{y}+\boldsymbol{W}t,t)\rangle\,\mathrm{d}t \\ &= \frac{1}{\tau_v^2}\int \boldsymbol{R}(\boldsymbol{k})\mathrm{d}\boldsymbol{k}\int_{-\infty}^{0}\mathrm{e}^{\mathrm{i}\boldsymbol{k}\cdot\boldsymbol{W}t}\mathrm{d}t \\ &= \frac{\pi}{\tau_v^2}\int \boldsymbol{R}(\boldsymbol{k})\delta(\boldsymbol{k}\cdot\boldsymbol{W})\mathrm{d}\boldsymbol{k}. \end{aligned} \tag{2.63}$$

Here, $\boldsymbol{W}$ represents the velocity of large-scale eddies that are advecting a frozen turbulent flow field past the particle. Using a procedure similar to that in (2.31)–(2.34), we get:

$$D_{v,ij}(W) = \frac{\pi}{\tau_v^2}\frac{1}{W}\int_0^\infty \xi\,\mathrm{d}\xi\int_0^{2\pi}\frac{E(\xi)}{4\pi\xi^2}\left(\delta_{ij}-\frac{\xi_i\xi_j}{\xi^2}\right)\mathrm{d}\phi. \tag{2.64}$$

We can write for isotropic turbulence:

$$D_{v,ij} = D_{v,\perp}\left(\delta_{ij}-\frac{r_ir_j}{r^2}\right)+D_{v,\parallel}\frac{r_ir_j}{r^2} \tag{2.65}$$

where $\boldsymbol{r}=\boldsymbol{v}t$. Using a procedure similar to the one laid out in § 2.3.1:

$$D_{v,\perp} = \frac{1}{2}D_{v,ij}\left(\delta_{ij}-\frac{r_ir_j}{r^2}\right) = \frac{\pi}{4\tau_v^2}\frac{1}{v}(2A+A\sin^2\theta), \tag{2.66}$$

$$D_{v,\parallel} = D_{v,ij}\frac{r_ir_j}{r^2} = \frac{\pi}{2\tau_v^2}\frac{1}{v}(A+A\cos^2\theta) \tag{2.67}$$

$$A = \frac{1}{2}\int_0^\infty \frac{E(\xi)}{\xi}\mathrm{d}\xi. \tag{2.68}$$

In order to remove the dependence on W, we perform weighted integration of $D_{v,\perp}$ and $D_{v,\parallel}$ using the PDF of $\boldsymbol{W}$, $\Phi(\boldsymbol{W})$, as follows:

$$D_{v,\perp} = \frac{\pi}{4\tau_v^2}\int\frac{1}{v}\left(2A+A\sin^2\theta\right)\Phi(\boldsymbol{W})\mathrm{d}\boldsymbol{W} \tag{2.69}$$

$$D_{v,\parallel} = \frac{\pi}{2\tau_v^2}\int\frac{1}{v}\left(A+A\cos^2\theta\right)\Phi(\boldsymbol{W})\mathrm{d}\boldsymbol{W}. \tag{2.70}$$

After performing the above integrations using $\Phi(\boldsymbol{W})$ from (2.28), it can be readily shown that

$$D_{v,\perp} = D_{v,\parallel} = \tfrac{1}{2}\lim_{r\to\infty}D_{UU,\perp} = \tfrac{1}{2}\lim_{r\to\infty}D_{UU,\parallel} \tag{2.71}$$

which is exactly the desired result, where $D_{UU,\perp}(r)$ and $D_{UU,\parallel}(r)$ are given by (2.49) and (2.50).

3. Simulations

Using the diffusion coefficient formulation derived in § 2, Lagrangian stochastic simulations were performed to evolve the pair separations ($\boldsymbol{r}$) and relative velocities ($\boldsymbol{U}$). The governing equations for $\boldsymbol{r}$ and $\boldsymbol{U}$ are:

$$\frac{\mathrm{d}\boldsymbol{r}}{\mathrm{d}t} = \boldsymbol{U}, \tag{3.1}$$

$$\mathrm{d}\boldsymbol{U} = -\frac{\boldsymbol{U}}{\tau_v}\mathrm{d}t + \boldsymbol{B}\cdot\mathrm{d}\boldsymbol{W}. \tag{3.2}$$

Here, $\boldsymbol{W}$ represents a Wiener process, and the diffusion matrix $\boldsymbol{B}$ can be written in terms of $\boldsymbol{D}_{UU}$ as:

$$\boldsymbol{B}\cdot\boldsymbol{B}^T = 2\boldsymbol{D}_{UU}(r) \tag{3.3}$$

where $\boldsymbol{B}^T$ is the transpose of $\boldsymbol{B}$, and $\boldsymbol{B}$ is computed from a Cholesky decomposition of $\boldsymbol{D}_{UU}(r)$. The matrix $\boldsymbol{B}$ is a function of the state variable $\boldsymbol{r}$. Consequently, the current Langevin model captures the deviation from Gaussianity with r of the PDF of $\boldsymbol{U}$. As discussed in Minier & Peirano (2001), in spite of the white-noise (Gaussian) treatment of the diffusion of the slow variable $\boldsymbol{U}$, the fact that the fast variable $\Delta\boldsymbol{u}$ contained in the diffusion coefficient depends upon the state variable $\boldsymbol{r}$ leads to the non-Gaussian behaviour of the slow variable.

In order to compute $\boldsymbol{D}_{UU}(r)$ and from it $\boldsymbol{B}$, we will need to evaluate the $\int_0^\infty$ integrals in (2.49) and (2.50). Numerical quadrature using the Gauss–Laguerre polynomials is ideally suited for these integrals. In our simulations, we used the 150th-order Gauss–Laguerre polynomials to evaluate these integrals. Although such high-order integration may not be needed, it was used since the additional computational expense was negligible. The isotropic turbulence energy spectrum function in (2.49) and (2.50) was evaluated using the following expression (Pope 2000):

$$E(k) = C\epsilon^{2/3}k^{-5/3}f_L(kL)\,f_\eta(k\eta) \tag{3.4}$$

where $C = 1.5$, ϵ is the turbulence dissipation rate, and f_L and f_η are functions of the integral and Kolmogorov length scales, L and η, respectively. Expressions for f_L and f_η are provided in Pope (2000) and are not reproduced here. The ratio $L/\eta \approx 156.5$ in our simulations.

Particle pairs were evolved in isotropic turbulence with a microscale Reynolds number, $Re_\lambda = 75$. Six particle Stokes numbers were considered: $St_\eta = \tau_v/\tau_\eta = 2, 4, 10, 20, 40$ and 80. For each St_η, we evolved the separations and relative velocities of 60×10^6 pairs. The particle simulation domain is a sphere of radius $4L$. It was found that this domain size was sufficiently large, since the separation at which particle pairs became uncorrelated was $O(L)$ for all Stokes numbers considered in the current study. As a result, a domain size of $4L$ is sufficient even for those uncorrelated pairs that have initially large separations and relative velocities, but become correlated as their separation decreases. For all St_η, the particle pairs were evolved for 8000 particle response times (τ_v) by which time they had attained a statistically stationary state. From this point, statistics were collected for another $1000\tau_v$ and averaged.

At the outer boundary, a specular reflection boundary condition (BC) was imposed for the particles. This meant that when a particle collides with the outer boundary, its velocity component tangential to the boundary remains unchanged, while the velocity component normal to the boundary is simply reversed. A specular reflection BC also maintains a constant number of pairs in the domain. In this sense, a domain with a specular reflection BC is analogous to a domain with a specified radially inward particle flux BC that has attained a steady state. This is because at steady state, a system with a specified inward particle flux BC will also have constant number of pairs in the domain. The other advantages of the specular reflection BC are that it conserves particle kinetic energy, and maintains a Gaussian particle velocity PDF at the far-field boundary.

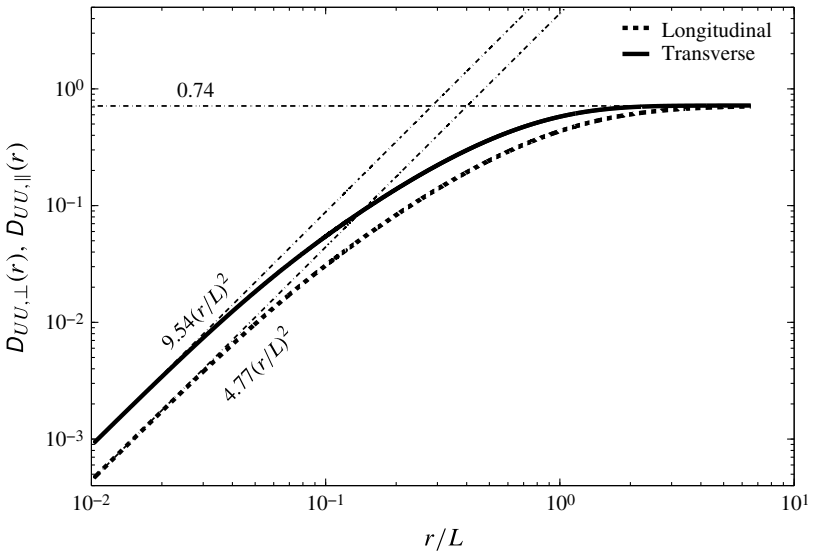

FIGURE 1. Transverse component, $D_{UU,\perp}(r)$, and longitudinal component, $D_{UU,\parallel}(r)$, of the particle-pair diffusion coefficient tensor as a function of dimensionless pair separation r/L for $St_\eta = 20$. Solid and dashed curves represent transverse and longitudinal components, respectively. At small r, transverse and longitudinal components asymptote to the lower and upper grey dashed lines represented by $4.77(r/L)^2$ and $9.54(r/L)^2$, respectively. At large r, transverse and longitudinal components asymptote to the value of 0.74.

It was found that encountering pairs with separations $r \sim \eta$ (η is the Kolmogorov length scale) were low-probability events. We, therefore, adopted the approach of Huber & Kim (1996) that facilitates the capturing of these low-probability events. In this approach, a single pair is split into multiple, equally weighted fractional pairs whenever the separation of a pair goes below a certain value. When a parent pair is split, initially the fractional pairs have the same position and velocity vectors as the parent. Each of the fractional pairs is then evolved independently, except that it only makes a fractional contribution when computing the statistics. In our simulations, splitting is executed at three different radial locations, $r = 2\eta$, 5η, 10η. A parent pair is split whenever the separation falls below any of these radial distances, but a fractional pair is not split again irrespective of whether the above criterion is satisfied or not. We found that splitting a pair into 10 equally weighted fractional pairs gave us sufficient data at the smaller separations without excessively increasing the number of pairs to be tracked. Recombination of fractional pairs when their separations exceeded the specified radial distances was not undertaken.

4. Results and discussion

In this section, the results obtained using the closure formulation derived in § 2 are discussed. First, we will present the transverse and longitudinal components of the diffusion coefficient tensor as a function of pair separation r. Subsequently, we will discuss in detail the particle statistics obtained from the Langevin simulations.

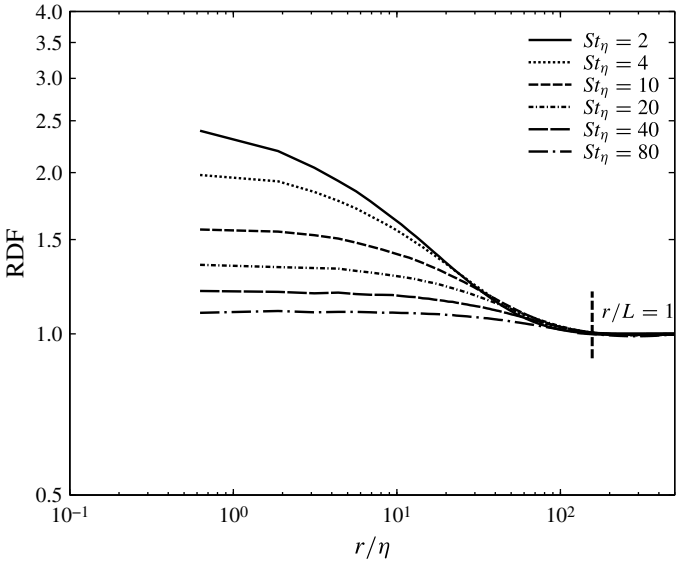

FIGURE 2. RDFs from our stochastic simulations for the various Stokes numbers as a function of dimensionless pair separation r/η. The radial location at which $r/L = 1$ is also indicated, where L is the integral length scale.

4.1. *Transverse and longitudinal components of the diffusion coefficient tensor*

The transverse and longitudinal components of the diffusion coefficient tensor plotted as a function of the dimensionless separation r/L are shown in figure 1 for the $St_\eta = 20$ particles. For separations $r < \eta$, both $D_{UU,\perp}(r)$ and $D_{UU,\parallel}(r)$ vary as r^2. This behaviour arises from (2.26) in conjunction with the fact that fluid relative velocity for $r < \eta$ can be approximated as a linear function of r, i.e. $\Delta \boldsymbol{u} \approx \boldsymbol{r} \cdot \boldsymbol{\nabla u}$ (Chun *et al.* 2005). It may be noted that the r-space diffusion coefficient for the small-Stokes-number particles ($St_\eta < 1$), which involves an autocorrelation of the fluid relative velocity, is also proportional to r^2 for $r < \eta$ (Chun *et al.* 2005). For $r \gtrsim L$, $D_{UU,\perp}(r)$ and $D_{UU,\parallel}(r)$ approach each other, and asymptote to the same limit. This means that when the separation r exceeds L, a particle pair essentially behaves like two uncorrelated particles, with the pair diffusion coefficient being twice that of a single particle (see the discussion in § 2.5). This trend is also supportive of our earlier assertion that a domain size of $4L$ was sufficiently large to capture those particle pairs that were initially uncorrelated at a large separation, but have subsequently become correlated as they moved closer. The other side of this picture is that we have also been able to show that pairs exhibit a transition from highly correlated motion at small separations to uncorrelated motion at larger separations.

4.2. *RDF and relative velocity PDF statistics*

In this section, we present the pair relative motion statistics obtained from the Langevin stochastic simulations. Figure 2 shows the RDFs as a function of the dimensionless separation r/η for the various Stokes numbers. At separations of the order of the Kolmogorov scale, the $St_\eta = 2$ particles show the maximum preferential concentration, i.e. the highest RDF values, among the Stokes numbers considered. Preferential concentration at separations $r \sim O(\eta)$ decreases with increasing Stokes

number. One also notes that for the higher Stokes numbers ($St_\eta \geqslant 10$), the RDFs plateau, i.e. they are essentially independent of r, below certain separations. A similar qualitative trend was seen in Zaichik & Alipchenkov (2003), but the plateauing was observed to begin at radial separations larger than those in the current study. The 'delayed' plateauing of RDFs observed in the current study is also qualitatively supported by the study of Pan *et al.* (2011). In that study, Pan *et al.* investigated the preferential concentration of high-Stokes-number particles in isotropic turbulence at $Re_\lambda = 250$. The higher Stokes numbers considered by Pan *et al.* include $St_\eta = 10, 21, 43$. The plateauing of RDFs can be explained using the transport equations for the moments of the PDF $\Omega(\boldsymbol{r}, \boldsymbol{U})$ (see (2.23)). The moments of interest are:

$$\Omega(\boldsymbol{r}) = \int \Omega(\boldsymbol{r}, \boldsymbol{U})\mathrm{d}\boldsymbol{U} = \Omega(\boldsymbol{r}) \int \Omega(\boldsymbol{U}|\boldsymbol{r})\mathrm{d}\boldsymbol{U}, \tag{4.1}$$

$$\langle \boldsymbol{U} \rangle = \int \boldsymbol{U}\Omega(\boldsymbol{U}|\boldsymbol{r})\mathrm{d}\boldsymbol{U} = \frac{1}{\Omega(\boldsymbol{r})} \int \boldsymbol{U}\Omega(\boldsymbol{r}, \boldsymbol{U})\mathrm{d}\boldsymbol{U} \tag{4.2}$$

where $\Omega(\boldsymbol{U}|\boldsymbol{r})$ is the PDF of $\boldsymbol{U}$ conditioned on a given $\boldsymbol{r}$.

The governing equation for $\Omega(\boldsymbol{r})$ is obtained by integrating (2.23) over the $\boldsymbol{U}$-space, and that for $\langle \boldsymbol{U} \rangle$ is obtained by premultiplying (2.23) with $\boldsymbol{U}/\Omega(\boldsymbol{r})$ and then integrating over the $\boldsymbol{U}$-space. The resulting equations, written using the Einstein index notation, are:

$$\frac{\partial \Omega(\boldsymbol{r})}{\partial t} + \frac{\partial [\Omega(\boldsymbol{r})\langle U_j \rangle]}{\partial r_j} = 0, \tag{4.3}$$

$$\frac{\partial \langle U_i \rangle}{\partial t} + \frac{\partial \langle U_i \rangle \langle U_j \rangle}{\partial r_j} + \frac{\partial \langle U_i' U_j' \rangle}{\partial r_j} = -\frac{\langle U_i \rangle}{\tau_v} - D_{ij} \frac{\partial \ln \Omega(\boldsymbol{r})}{\partial r_j}. \tag{4.4}$$

For isotropic turbulence, $\langle U_i \rangle = 0$, thereby (4.4) becomes

$$\frac{\partial \langle U_\alpha' U_\alpha' \rangle}{\partial r_j} = -D_{\alpha\alpha} \frac{\partial \ln \Omega(\boldsymbol{r})}{\partial r_j} \tag{4.5}$$

where $\alpha = 1, 2, 3$ (repeated α does not denote a summation). The relationship between $\Omega(r)$ and the RDF $g(r)$ is given by

$$g(r) = \frac{\Omega(r)}{\left[\dfrac{N(N-1)}{2V}\right]} \tag{4.6}$$

where N is the number of individual particles in the domain and V is the volume of the domain. One can therefore see from (4.5) that the plateauing of the RDF $g(r)$ is related to the plateauing of $\langle U_\alpha' U_\alpha' \rangle$. To confirm this, figure 3 plots $\langle U^2 \rangle / u_{rms}^2$ as a function of r/L for the various St_η, where u_{rms} is the turbulence r.m.s. fluctuating velocity. It is evident from figure 3 that for $St_\eta \geqslant 10$, $\langle U^2 \rangle$ indeed begins to plateau at smaller separations, with the trend being more evident for $St_\eta = 40, 80$. Consequently, following (4.5), a similar behaviour was also observed for the RDFs in figure 2.

RDF as a function of St_η at various separations r/η is presented in figure 4. Results from the current theory are compared with the DNS data of Février *et al.* (2001), and also with the results from the theory of Zaichik & Alipchenkov (2003). The Février

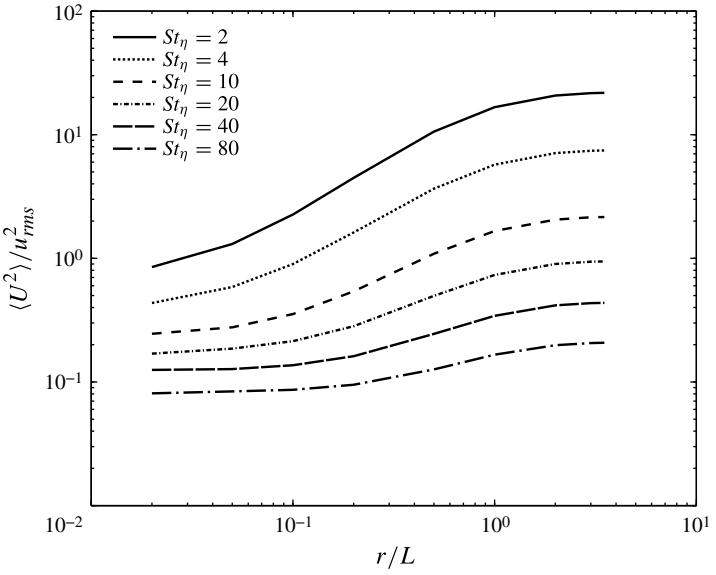

FIGURE 3. $\langle U^2 \rangle / u_{rms}^2$ as a function of dimensionless pair separation r/L and particle Stokes number St_η.

et al. (2001) data were for $Re_\lambda = 53$ and $Re_\lambda = 69$, while the Zaichik & Alipchenkov (2003) results were for $Re_\lambda = 75$. There is reasonable agreement between the current theory and the DNS (note that $Re_\lambda = 75$ in the current study). For $St_\eta \geqslant 2$, this theory agrees better with the DNS data than does the theory of Zaichik & Alipchenkov (2003). This may be attributed to the approximation in their study that the Lagrangian correlations of fluid relative velocities along inertial-pair trajectories are equal to those along inertialess fluid particle-pair trajectories. Such an approximation is only appropriate for particle Stokes numbers $St_\eta < 1$. It can be inferred from figure 4(*c*,*d*) that as the separation r increases, the Stokes number for which the maximum RDF occurs also increases. This is because the higher-Stokes-number particles are more responsive to eddies bigger than the Kolmogorov-sized ones, and hence these pairs exhibit preferential concentration at length scales larger than the Kolmogorov scale.

Next, we discuss the pair relative-velocity PDF and its moments obtained from our Langevin simulations. The DNS study of Sundaram & Collins (1997) demonstrated that the relative-velocity PDF is Gaussian at separations of the order of the integral length scale, and that it becomes increasingly non-Gaussian, tending towards exponential, as the separation decreases. It is important that the present theory captures this trend. The transition in the nature of the PDF can be demonstrated quantitatively using the relative-velocity kurtosis $\langle U^4 \rangle / \langle U^2 \rangle^2$. It is well known that the kurtosis $= 3$ for a Gaussian PDF, and a deviation from this value is indicative of a non-Gaussian PDF. In figure 5, kurtosis is plotted as a function of r/L for the various St_η. When $r \gtrsim L$, the relative-velocity PDFs for all Stokes numbers are essentially Gaussian. As the separation decreases, kurtosis increases above 3. This trend is more prominent at the smaller St_η because these particles relax to the local flow conditions, whereas the higher-St_η particles still retain memory of their ballistic motion at prior larger separations. It is interesting to note that at $r/L \approx 1/20$, the kurtosis ≈ 9 for the $St_\eta = 4$ particles, suggesting that at this radial separation, the relative velocities

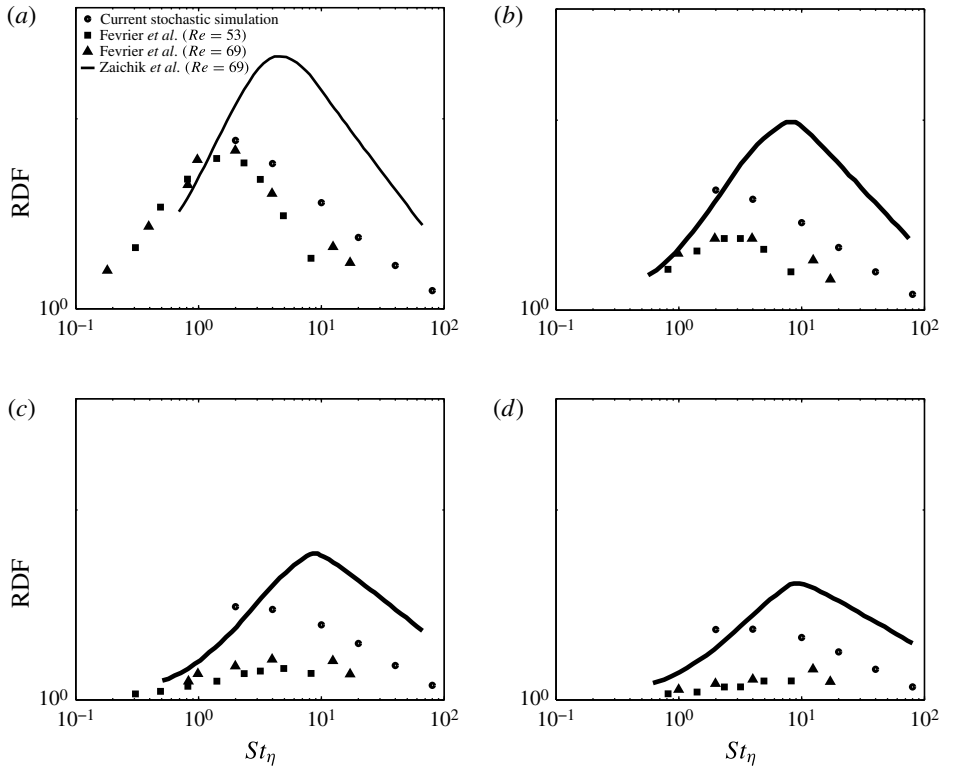

FIGURE 4. RDF versus St_η at specific radial separations: (*a*) $r/\eta = 6$, (*b*) $r/\eta = 12$, (*c*) $r/\eta = 18$, and (*d*) $r/\eta = 24$. In each plot, circles represent data from current stochastic simulations at $Re_\lambda = 75$; squares and triangles represent DNS data at $Re_\lambda = 53$ and $Re_\lambda = 69$, respectively, taken from Février *et al.* (2001); solid line represents Zaichik & Alipchenkov (2003) data for $Re_\lambda = 69$.

of these particles have a nearly exponential distribution. But, as the separation falls below $L/20$, kurtosis increases further implying that the relative velocities of the $St_\eta = 4$ pairs no longer have an exponential distribution. The separation at which the exponential distribution is attained decreases as the Stokes number increases.

Another interesting aspect of physics that can be gleaned from the relative-velocity statistics is regarding the Stokes-number dependence of pair relative-velocity variance $\langle U^2 \rangle$. For high-St_η particles, it is known that the single-particle velocity variance $\langle v^2 \rangle \propto 1/St$. Also, we have shown in § 2.5 that a pair at infinite separation behaves like two independent particles. These two aspects would mean that for large r, $\langle U^2 \rangle St_\eta$ should become independent of both St_η and r. This is precisely what we observe in figure 6. In this figure, we plot $(\langle U^2 \rangle St_\eta)/u_{rms}^2$ as a function of r/L for various St_η, where u_{rms} is the turbulence r.m.s. fluctuating velocity. For $St_\eta \geqslant 20$, $(\langle U^2 \rangle St)/u_{rms}^2$ asymptotes to nearly the same value at large r. The lower-St_η pairs show a greater variation of variance with radial position. This is because the faster relaxation of the low-St_η particles makes it easier for them to get trapped and linger near each other.

Relative-velocity PDFs conditioned on the separation r, $\Omega(U|r)$, are presented for all St_η at $r/L = 3, 1, 1/10, 1/20$ (here $\eta/L = 0.0064$). These values of pair separation

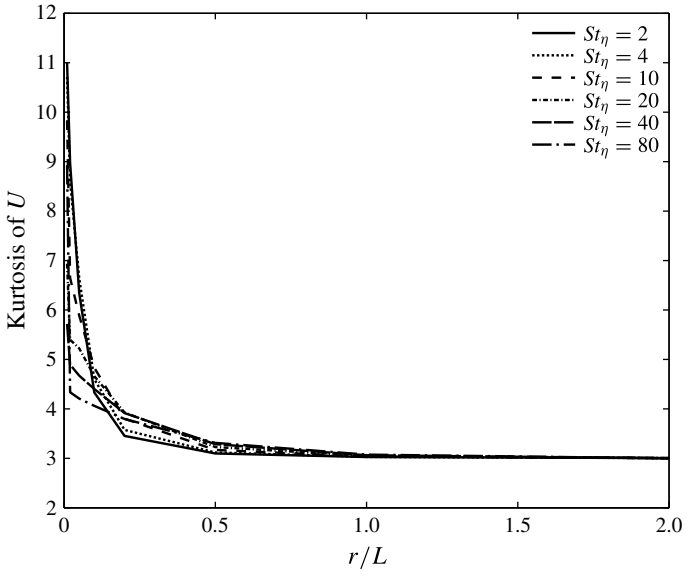

FIGURE 5. Kurtosis for various Stokes numbers as a function of dimensionless pair separation r/L.

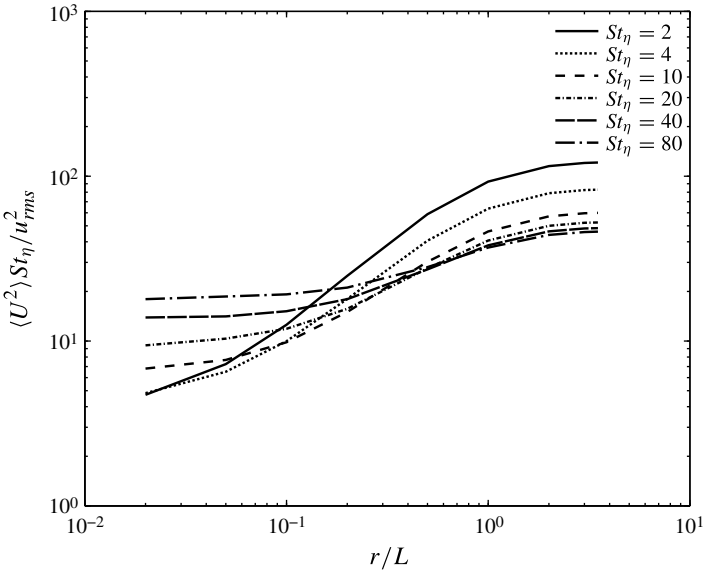

FIGURE 6. $\langle U^2 \rangle / u_{rms}^2$ as a function of dimensionless pair separation r/L and particle Stokes number St_η.

were chosen in order to track the transition of $\Omega(U|r)$ from a Gaussian PDF at large r to a non-Gaussian PDF at small r. Shown in figure 7(*a–d*) are the PDFs at these four values of r plotted as a function of the relative velocity magnitude U normalized with $\langle U^2 \rangle^{1/2}$ at that value of r. At each r, we compare the PDFs for all the St_η under consideration in this study. It can be seen in figure 7(*a*,*b*) that the PDFs

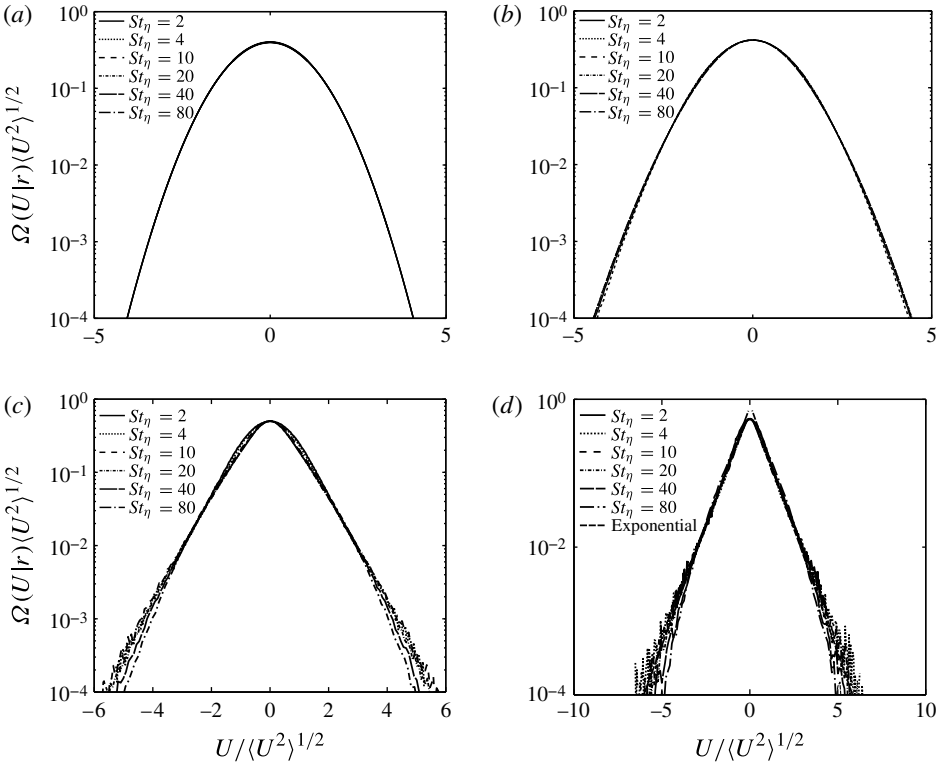

FIGURE 7. Relative velocity PDFs ($\Omega(U)$) for the various Stokes numbers at specific separations: (*a*) $r/L = 3$, (*b*) $r/L = 1$, (*c*) $r/L = 1/10$, (*d*) $r/L = 1/20$.

at $r/L = 3, 1$ are Gaussian for all St_η, and that there is a near-perfect collapse of the PDFs for the various Stokes numbers. This collapse of PDFs when normalized by the standard deviation is to be expected for Gaussian PDFs. Figure 7(*c*) shows that at $r/L = 1/10$, the PDFs for all St_η deviate from being Gaussian. As we reduce the pair separation to $r/L = 1/20$, the non-Gaussianity of the PDFs increases, particularly for the smaller St_η. This is because the smaller-St_η particles relax to the local flow, whereas the higher-St_η particles still retain some memory of their earlier ballistic motion at larger separations. Also shown in figure 7(*d*) is the exponential distribution. It is clear that the relative-velocity PDFs are very nearly exponential, especially for $St_\eta \leqslant 10$, and seem to deviate from it only at the higher values of U. The transition of the PDFs, as well as their exponential nature at smaller separations, match the trends observed in the DNS study of Sundaram & Collins (1997).

Thus, it is clear from figure 7 that when $r \gtrsim L$, particles become uncorrelated leading to Gaussian relative-velocity PDFs. As r goes below L, particles become correlated giving rise to exponential PDFs for certain separations. Eventually, as r approaches η, the pairs can be classified into 'lingerers' with low relative velocities, and 'flyers' with high relative velocities (corresponding to the tails of the PDF). Also, we show in figure 8 the PDF $\Omega(U|r)$ as a function of U at various separations r for $St_\eta = 20$. The transition in $\Omega(U|r)$ from being Gaussian at large r ($O(L)$) to being nearly exponential at small r is evident in this figure.

We will now focus on the radial component of the relative velocity $U_r = \boldsymbol{U}\cdot\boldsymbol{r}/r$ and its PDF. The significance of U_r lies in the role it plays in determining the interparticle

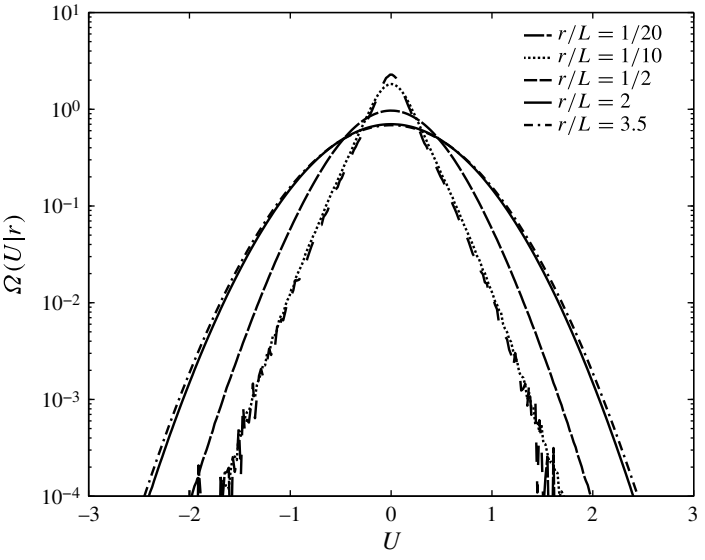

FIGURE 8. Comparison of relative velocity PDFs at various pair separations for $St_\eta = 20$.

collision rate. This is quantitatively illustrated by the collision kernel which for a monodisperse population of particles can be written as (Sundaram & Collins 1997; Wang, Wexler & Zhou 2000):

$$4\pi\sigma^2 g(\sigma) \int_{-\infty}^{0} U_r P(U_r|\sigma) \mathrm{d}U_r, \tag{4.7}$$

where σ is the particle diameter, $g(\sigma)$ is the RDF at contact, and $P(U_r|\sigma)$ is the PDF of U_r conditioned upon a particle separation $r = \sigma$. Figure 9 shows the PDF of U_r for the various Stokes numbers at $r/L = 1/20$. It is clear that U_r is negatively skewed, which is qualitatively consistent with the DNS study of Wang *et al.* (2000). Further, the skewness of U_r increases as the Stokes number decreases.

5. Summary and conclusions

The principal contributions of this study are twofold: (i) derivation of a novel closure for the relative-velocity-space pair diffusion coefficient for particle pairs whose Stokes numbers $St_r \gg 1$; and (ii) relaxation of the limitation on Stokes numbers so that the theory is valid for $St_I \lesssim 1$ particles as well. This relaxation significantly expands the Stokes number range in which the closure is applicable. In fact, the results demonstrate that the theory shows good predictions for $St_\eta \geqslant 4$.

The closure formulation was motivated by a DNS study result that the PDF of particle-pair relative velocity of inertial particles was Gaussian at pair separations of the order of turbulent integral length scale, and that this PDF became non-Gaussian (exponential) at smaller separations (Sundaram & Collins 1997). The salient feature in this closure is that Lagrangian two-time, two-point fluid velocity correlations are systematically and consistently transformed into Eulerian two-point correlations in the limit of high Stokes number.

In the present study, the theory-predicted diffusion tensor is used to evolve, in a Langevin sense, the pair separation and velocity vectors in isotropic turbulence. When

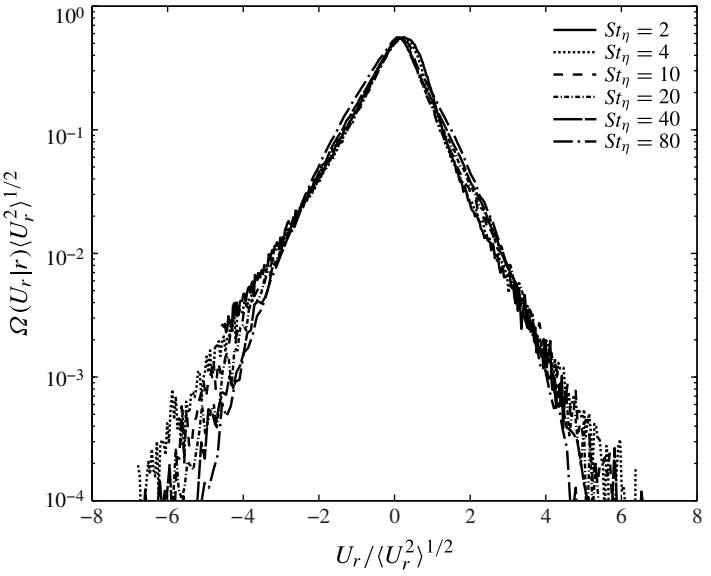

FIGURE 9. PDF of the radial component of the relative velocity U_r for the various Stokes numbers at $r/L = 1/20$.

compared to solving a finite number of PDF moments equations, this approach is higher-order accurate in the sense that the Langevin simulations implicitly include all moments of the pair PDF. The range of Stokes numbers considered, $St_\eta = 2$, 4, 10, 20, 40 and 80, clearly demonstrates the relative-velocity dynamics and the preferential concentration behaviour of high-Stokes-number particles. The closure theory successfully captures the transition of relative-velocity PDF from a Gaussian PDF at separations of the order of the integral length scale to an exponential PDF at smaller separations. This study is only an initial step in the effort to develop a predictive stochastic model for inertial-particle dynamics. A more thorough quantitative evaluation of our theory using DNS data will be undertaken in a future study.

Acknowledgements

D.L.K. acknowledges support from NSF grant CTS-1233793.

Appendix A. PDF notation used in the current study

The following notations are used in the manuscript:

(i) P is the particle-pair phase-space density.
(ii) $\langle P\rangle$ is the PDF.

The particle-pair microscopic PSD may be written as

$$f(\boldsymbol{r}, \boldsymbol{x}, \boldsymbol{U}, \boldsymbol{V}; t) = \sum_{i=1}^{N} \delta(\boldsymbol{r} - \boldsymbol{r}_i)\delta(\boldsymbol{x} - \boldsymbol{x}_i)\delta(\boldsymbol{V} - \boldsymbol{V}_i)\delta(\boldsymbol{U} - \boldsymbol{U}_i) \tag{A 1}$$

where $\boldsymbol{r}_i$, $\boldsymbol{x}_i$, $\boldsymbol{V}_i$, and $\boldsymbol{U}_i$ are the separation, centre-of-mass position, centre-of-mass velocity, and the relative velocity vectors of the ith pair, and N is the total number of pairs.

We now consider a smoothed PSD defined as

$$P(\boldsymbol{r}, \boldsymbol{x}, \boldsymbol{U}, \boldsymbol{V}; t) = \frac{1}{v} \int_v f(\boldsymbol{r}' - \boldsymbol{r}, \boldsymbol{x}' - \boldsymbol{x}, \boldsymbol{U}' - \boldsymbol{U}, \boldsymbol{V}' - \boldsymbol{V}; t) \mathrm{d}\boldsymbol{r}' \mathrm{d}\boldsymbol{x}' \mathrm{d}\boldsymbol{U}' \mathrm{d}\boldsymbol{V}'. \tag{A 2}$$

Here, the volume of integration v is a subvolume around $(\boldsymbol{r}, \boldsymbol{x}, \boldsymbol{U}, \boldsymbol{V})$ that is small compared to the corresponding Kolmogorov scales, but is sufficiently large to ensure that one is able to define a meaningful averaged quantity over v. Consequently, the averaging does not affect the fluid quantities so that there are no 'subgrid'-scale fluctuations.

The smoothed PSD P takes on added significance when there exists an irreversible process that causes particles to lose memory of their initial conditions. If particle motion exhibits deterministic chaos, then there is an exponential separation of trajectories with nearly identical initial conditions. Even a single realization of the turbulent flow leads to Lagrangian chaos for particle motion due to the nonlinear dependence of the velocity on position. In this case, a very small stochastic displacement of the particles can lead to the mixing of PSD over volumes of order v so that f approaches P. In the present situation, the small stochastic element could be the Brownian displacements of the particles. Although the Péclet number Pe of high-St particles is large ($O(10^5$–$10^6)$), the time required for mixing in the phase space is only proportional to $\tau \ln(Pe)$, where τ is the flow time scale corresponding to the length scale within v. Thus, in practice even a very small-scale stochastic process can lead to a smooth PSD. The smoothing of PSD also plays an important role in kinetic theory and in statistical mechanical approaches to classical molecular systems. In such systems, the Newton's equations of motion that govern the system are deterministic (even including collisions) and it is only the small quantum effects that lead to a stochastic element. Nonetheless, the deterministic chaotic motion of the molecules leads to rapid amplification of these stochastic effects so that stochastically averaged approaches are useful.

REFERENCES

Ayala, O., Rosa, B. & Wang, L.-P. 2008 Effects of turbulence on the geometric collision rate of sedimenting droplets. Part 2. Theory and parameterization. *New J. Phys.* **10**, 1–40.

Batchelor, G. K. 1953 *The Theory of Homogeneous Turbulence*. Cambridge University Press.

Bixon, M. & Zwanzig, R. 2005 Boltzmann–Langevin equation and hydrodynamic fluctuations. *Phys. Rev.* **187**, 267–272.

Bragg, A., Swailes, D. C. & Skartlien, R. 2012 Drift-free kinetic equations for turbulent dispersion. *Phys. Rev.* E **86**, 056306.

Buyevich, Yu. A. 1971 Statistical hydromechanics of disperse systems. Part 1. Physical background and general equations. *J. Fluid Mech.* **49**, 489–507.

Buyevich, Yu. A. 1972*a* Statistical hydromechanics of disperse systems. Part 2. Solution of the kinetic equation for suspended particles. *J. Fluid Mech.* **52**, 345–355.

Buyevich, Yu. A. 1972*b* Statistical hydromechanics of disperse systems. Part 3. Pseudo-turbulent structure of homogeneous suspensions. *J. Fluid Mech.* **56**, 313–336.

Chiang, E. & Youdin, A. 2005 Forming planetesimals in solar and extrasolar nebulae. *Annu. Rev. Earth Planet. Sci.* **38**, 493–522.

Chun, J., Koch, D. L., Rani, S. L., Ahluwalia, A. & Collins, L. R. 2005 Clustering of aerosol particles in isotropic turbulence. *J. Fluid Mech.* **536**, 219–251.

DEREVICH, I. V. 2006 Statistical modeling of particles relative motion in a turbulent gas flow. *Intl J. Heat Mass Transfer* **49**, 4290–4304.

DRUZHININ, O. A. 1995 On the two-way interaction in two-dimensional particle-laden flows: the accumulation of particles and flow modification. *J. Fluid Mech.* **297**, 49–76.

DRUZHININ, O. A. & ELGHOBASHI, S. 1999 On the decay rate of isotropic turbulence laden with microparticles. *Phys. Fluids* **11**, 602–610.

EATON, J. K. & FESSLER, J. R. 1994 Preferential concentration of particles by turbulence. *Intl J. Multiphase Flow* **20**, 169–209.

FERRY, J. & BALACHANDAR, S. 2001 A fast Eulerian method for disperse two-phase flow. *Intl J. Multiphase Flow* **27**, 1199–1226.

FERRY, J., RANI, S. L. & BALACHANDAR, S. 2003 A locally implicit improvement of the equilibrium Eulerian method. *Intl J. Multiphase Flow* **29**, 869–891.

FÉVRIER, P., SIMONIN, O. & LEGENDRE, D. 2001 Particle dispersion and preferential concentration dependence on turbulent Reynolds number from direct and large-eddy simulations of isotropic homogeneous turbulence. In *Proceedings of the Fourth International Conference on Multiphase Flow, New Orleans*.

GARDINER, C. W. 1990 *Handbook of Stochastic Methods for Physics, Chemistry and the Natural Sciences*. Springer.

GOSWAMI, P. S. & KUMARAN, V. 2010*a* Particle dynamics in a turbulent particle-gas suspension at high Stokes number. Part 1. Velocity and acceleration distributions. *J. Fluid Mech.* **646**, 59–90.

GOSWAMI, P. S. & KUMARAN, V. 2010*b* Particle dynamics in a turbulent particle-gas suspension at high Stokes number. Part 2. The fluctuating-force model. *J. Fluid Mech.* **646**, 91–125.

GUALTIERI, P., CASCIOLA, C. M., BENZI, R., AMATI, G. & PIVA, R. 2002 Scaling laws and intermittency in homogeneous shear flow. *Phys. Fluids* **14** (2), 583–596.

HUBER, G. A. & KIM, S. 1996 Weighted-ensemble Brownian dynamics simulations for protein association reactions. *Biophys. J.* **70**, 97–110.

HYLAND, K. E., MCKEE, S. & REEKS, M. W. 1999 Derivation of a pdf kinetic equation for the transport of particles in turbulent flows. *J. Phys. A: Math. Gen.* **32**, 6169–6190.

JUNG, J., YEO, K. & LEE, C. 2008 Behavior of heavy particles in isotropic turbulence. *Phys. Rev.* E **77**, 016307.

KELLY, G. E. & LEWIS, M. B. 1971 Hydrodynamic fluctuations. *Phys. Fluids* **14** (9), 1925–1931.

KOCH, D. L. 1990 Kinetic theory for a monodisperse gas–solid suspension. *Phys. Fluids* **2** (10), 1711–1723.

KRAICHNAN, R. H. 1961 Dynamics of nonlinear stochastic systems. *J. Math. Phys.* **2**, 124–148.

KRAICHNAN, R. H. 1965 Lagrangian-history closure approximation for turbulence. *Phys. Fluids* **8** (4), 575–598.

MAXEY, M. R. 1987 The gravitational settling of aerosol particles in homogeneous turbulence and random flow fields. *J. Fluid Mech.* **174**, 441–465.

MINIER, J.-P. & PEIRANO, E. 2001 The pdf approach to turbulent polydispersed two-phase flows. *Phys. Rep.* **352**, 1–214.

MORI, H. 1973*a* Kinetic equations for the particle density in μ space. *Prog. Theor. Phys.* **49**, 357–358.

MORI, H. 1973*b* Statistical-mechanical theory of kinetic equations. *Prog. Theor. Phys.* **49**, 1516–1545.

ONUKI, A. 1978 On fluctuations in μ space. *J. Statist. Phys.* **18** (5), 475–499.

PAN, L. & PADAON, P. 2010 Relative velocity of inertial particles in turbulent flows. *J. Fluid Mech.* **661**, 73–107.

PAN, L., PADOAN, P., SCALO, J., KRITSUK, A. G. & NORMAN, M. L. 2011 Turbulent clustering of protoplanetary dust and planetesimal formation. *Astrophys. J.* **740**, 1–21.

PANDYA, R. V. R. & MASHAYEK, F. 2003 Non-isothermal dispersed phase of particles in turbulent flow. *J. Fluid Mech.* **475**, 205–245.

POPE, S. B. 2000 *Turbulent Flows*. Cambridge University Press.

POZORSKI, J. & MINIER, J.-P. 1999 Probability density function modeling of dispersed two-phase turbulent flows. *Phys. Rev.* E **59**, 855–863.

RANI, S. L. & BALACHANDAR, S. 2003 Evaluation of the equilibrium Eulerian approach for the evolution of particle concentration in isotropic turbulence. *Intl J. Multiphase Flow* **29**, 1793–1816.

RAY, B. & COLLINS, L. R. 2011 Preferential concentration and relative velocity statistics of inertial particles in Navier–Stokes turbulence with and without filtering. *J. Fluid Mech.* **680**, 488–510.

READE, W. C. & COLLINS, L. R. 2000 Effect of preferential concentration on turbulent collision rates. *Phys. Fluids* **12** (10), 2530–2540.

REEKS, M. W. 1980 Eulerian direct interaction applied to the statistical motion of particles in a turbulent flow. *J. Fluid Mech.* **97**, 569–590.

REEKS, M. W. 1991 On a kinetic equation for the transport of particles in turbulent flows. *Phys. Fluids* A **3** (3), 446–456.

REEKS, M. W. 1992 On the continuum equations for dispersed particles in nonuniform flows. *Phys. Fluids* A **4**, 1290–1303.

REEKS, M. W. 2005 On probability density function equations for particle dispersion in a uniform shear flow. *J. Fluid Mech.* **522**, 263–302.

SHOTORBAN, B. 2011 Preliminary assessment of two-fluid model for direct numerical simulation of particle-laden flows. *AIAA J.* **49**, 438–443.

SIMONIN, O., DEUTSCH, E. & MINIER, J.-P. 1993 Eulerian prediction of the fluid/particle correlation motion in turbulent two-phase flows. *Appl. Sci. Res.* **51**, 275–283.

SQUIRES, K. D. & EATON, J. K. 1991 Preferential concentration of particles by turbulence. *Phys. Fluids* A **3**, 1169–1178.

SUNDARAM, S. & COLLINS, L. R. 1997 Collision statistics in an isotropic particle-laden turbulent suspension. Part 1. Direct numerical simulations. *J. Fluid Mech.* **335**, 75–109.

SWAILES, D. C. & DARBYSHIRE, K. F. F. 1997 A generalized Fokker–Planck equation for particle transport in random media. *Physica* A **242**, 38–48.

WANG, L.-P., WEXLER, A. S. & ZHOU, Y. 2000 Statistical mechanical description and modelling of turbulent collision of inertial particles. *J. Fluid Mech.* **415**, 117–153.

ZAICHIK, L. I. & ALIPCHENKOV, V. M. 2003 Pair dispersion and preferential concentration of particles in isotropic turbulence. *Phys. Fluids* **15**, 1776–1787.

ZAICHIK, L. I. & ALIPCHENKOV, V. M. 2007 Refinement of the probability density function model for preferential concentration of aerosol particles in isotropic turbulence. *Phys. Fluids* **19**, 113308.

ZAICHIK, L. I., SIMONIN, O. & ALIPCHENKOV, V. M. 2003 Two statistical models for predicting collision rates of inertial particles in homogeneous isotropic turbulence. *Phys. Fluids* **15**, 2995–3005.

ZAICHIK, L. I., SIMONIN, O. & ALIPCHENKOV, V. M. 2006 Collision rates of bidisperse inertial particles in isotropic turbulence. *Phys. Fluids* **18**, 1–13.